

FAMAC: A Federated Assisted Modified Actor-Critic Framework for Secured Energy Saving in 5G and Beyond Networks

Attai Ibrahim Abubakar^{*†}, Michael S. Mollel^{†‡}, Naeem Ramzan^{*}

Abstract—The constant surge in the traffic demand on cellular networks has led to continuous expansion in network capacity in order to accommodate existing and new service demands. This has given rise to ultra-dense base station deployment in 5G and beyond networks which leads to increased energy consumption in the network. Hence, these ultra-dense base station deployments must be operated in a way that the energy consumption of the network can be adapted to the spatio-temporal traffic demands on the network in order to minimize the overall energy consumption of the network. To achieve this goal, we leverage two artificial intelligence algorithms, federated learning and actor-critic algorithm, to develop a proactive and intelligent base station switching framework that can learn the operating policy of the small base station in an ultra-dense heterogeneous network (UDHN) that would result in maximum energy saving in the network while respecting the quality of service (QoS) constraints. The performance evaluation reveals that the proposed framework can achieve an energy saving that is about 77% more than that of the state-of-the-art solutions while respecting the QoS constraints of the network.

Index Terms—Energy-efficient Wireless Communications, Power Consumption Modelling, Energy Optimization, Federated Learning, Reinforcement Learning, 5G and Beyond Networks.

I. INTRODUCTION

The need to minimize the energy consumption of cellular networks is a major challenge that must be addressed to reduce the operating expenditure of mobile network operators (MNOs) and achieve environmental sustainability [1]. With the growing demands for enhanced data rates for social media applications, online gaming, virtual and augmented reality platforms, massive connectivity of handheld and machine-type devices, the MNOs have to embrace network densification involving the enormous deployment of different types of base stations (BSs) including macro, micro, pico, femto BSs to provide enhanced capacity, coverage, and high data rate transmission, particularly in urban areas [2]–[4]. One of the negative consequences of the ultra-dense deployment of BSs is a surge in the energy consumption of the network [5], [6]. Hence, there is a need for intelligent frameworks to be developed to efficiently manage this massive network deployment in 5G and beyond networks so that the gains achieved due to network densification in the form of enhanced capacity and

coverage are not overwhelmed by the escalation in energy consumption.

Several approaches have already been proposed in the literature for optimizing the energy consumption of cellular networks from efficient hardware design [7], to transmit power allocation and controls [8], carrier shutdown [9], dynamic sector switching [10], various sleep mode operations, and dynamic BSs switching off/on [11], [12]. The dynamic switching off/on of BSs is still one of the most widely accepted methods for achieving maximum energy optimization as it tries to ensure that the energy consumed by the BSs scales with the traffic demand on the network and can be easily implemented without much changes to the network architecture [13], [14]. In addition, the energy saving achieved by other methods is not as significant as that of the BS switch-off/on method because it has been discovered in the literature that a significant amount of energy is consumed by the BS even when it is not serving any user request for control functionalities [15].

Even though the BS switching off/on is one of the best solutions to achieving maximum energy saving, the challenges involved in implementing this approach from an algorithm perspective have been a major hindrance preventing its adoption in real-life networks. It has been proven in [16] that the BSs switching problem is a combinatorial optimization problem which is NP-hard due to the fact that the number of possible search spaces to select the optimal solutions grows exponentially with the number of BSs deployed in the network. As such, for large-scale network deployment, the number of search spaces can grow extremely large, thus making it difficult to find suitable algorithms that can be used to find the optimal solutions for such combinatorial problems. Exhaustive search or brute force algorithm is the only algorithm always guaranteed to find the optimal solution. However, it encounters substantial computational overhead when the network size becomes enormous and as such, it is only suitable for small network deployments [17]. Hence, a near-optimal solution with much lesser computation overhead is often resorted to to enable the solution to scale with the network size. Heuristics, meta-heuristic, and machine learning-based solutions have been proposed to find near-optimal solutions. However, some of the solutions developed still suffer from colossal computation overhead and are not adaptable to dynamically changing network traffic conditions. In addition, most of them require regular sharing of traffic information among the BSs to find the optimal solution, which raises security concerns and the possibility of compromising the data privacy of the users in the

^{*}School of Computing, Engineering and Physical Sciences, University of the West of Scotland, Paisley, UK. [†]James Watt School of Engineering, University of Glasgow, UK. [‡] Nelson Mandela African Institute of Science and Technology Arusha, Arusha, TZ. Corresponding Email: attai.abubakar@glasgow.ac.uk.

TABLE I
TABLE OF NOTATIONS

Symbol	Meaning
$\sigma_{x,j}$	User transmission rate
ζ_x	No. of RB assigned to user x
κ_{RB}	Bandwidth of one RB
$\gamma_{x,j}$	Signal-to-noise-plus-interference-ratio
Φ_x	Minimum data rate of user x
$N_{x,j}$	Number of RB required to meet
P_{BS}	Instantaneous BS power consumption
P_o	BS fixed power consumption
μ	Amplifier efficiency
P_{tx}	BS transmission power
P_s	Sleep power consumption
ψ	BS instantaneous traffic load
P_{max}	Maximum power consumption
N_m	Total number of macro cell
N_b	Total number of BS in each BS
N_T	Number of time slots
Φ^i	Traffic demand of the MC before traffic offloading
χ^i	Traffic demand of the MC after traffic offloading
$\Gamma_t^{i,j}$	Off/on state of the j^{th} BS in the i^{th} MC
N_T	Number of time slots
L	Duration of time slots
R_T	Cumulative discount reward
s_t	state
a_t	action set
C_l	coverage loss

network. There is also the problem of high signaling overhead which leads to increased bandwidth consumption [6], [18].

We propose a Federated-Assisted Modified Actor-Critic (FAMAC) reinforcement learning (RL)-based energy optimization framework for ultra-dense 5G and beyond networks. The framework involves two stages: In the first stage, federated learning is applied to determine the traffic prediction model of each small BS in the network. These prediction models are then shared with the central controller. The central controller constructs a look-up table with the models where the instantaneous traffic demands of each small BSs (SBS) can be easily obtained, rather than having each SBS continually send its traffic demand to the macro BS (MBS) whenever a switching decision is to be made. The second stage involves learning the optimal switching strategy to minimise energy consumption using a modified version of the actor-critic DRL. The conventional actor-critic DRL algorithms have the challenge of dealing with combinatorial problems with large discrete action spaces as obtained in the BS switching problem, and this may lead to slow convergence, degraded or infeasible solutions [19]. In the modified actor-critic deep reinforcement algorithm, we adjust the internal architecture of the actor in such a way that would enable it to handle problems with large action spaces, as is the case with BS switch-off/on in ultra-dense networks. In addition, we introduce both global and local weights, where the global weights facilitate cooperation among the various SBSs traffic parameters while the local weights are meant to learn features peculiar to the network condition at individual SBSs in the network. This modification equips the actor-critic DRL algorithm to determine the optimal solution even when the number of discrete action spaces becomes significantly huge.

A. Paper Organization

The remaining parts of the paper are organized as follows: a review of the state-of-the-art approaches applied for dynamic BS switching off/on is presented in section II, while section III presents the system model, which comprises the Network model, BS load model power consumption model and section IV presents the problem formulation and optimization objective. The proposed framework's methodology is detailed in section V, while section VI presents the performance evaluation of the proposed and benchmark methods. The paper is concluded in Section VII.

II. RELATED WORKS

Several algorithmic approaches ranging from heuristics, meta-heuristics, and machine learning algorithms have been employed to determine the optimal or sub-optimal BS switching decision in order to minimize the energy consumption of cellular networks. In terms of heuristic and meta-heuristic algorithms, simulated annealing algorithm [20]–[22], particle swarm optimization [23]–[25], sorting algorithms [26], [27], genetic algorithm [28], [29], etc have been proposed for BS switch-off/on in the literature. The problem with heuristic and meta-heuristic approaches is that they are executed with conditional statements, find it difficult to generalize to unseen observations, and cannot easily adapt to a dynamically changing network condition as obtained in ultra-dense 5G and beyond networks. In addition, due to the dynamic changes in the network, there is a need to apply these solutions to calculate the optimal solution each time the network condition changes, which results in increased computational overhead. As a result, most times, before the computation of the optimal solution is completed and the decision implemented, the condition of the network would have changed, thereby leading to the generation of sub-optimal results. The effect of this on the QoS of the network is increased delays and service failure. Hence, most of them are unsuitable for BS to switch off/on in ultra-dense 5G and beyond networks as they can lead to poor QoS and sub-optimal network performance [30], [31].

The other approach to BS switching is machine learning solutions which are able to learn from historical data or real-time environments some hidden features that heuristic and meta-heuristic algorithms cannot capture. In addition, they do not have to be explicitly programmed with conditional statements before finding the near-optimal solution. As a result, they can adapt to dynamically changing network configurations in order to learn a near-optimal solution. In this regard, supervised learning algorithms (neural networks [32]–[35]), unsupervised learning algorithms (clustering algorithms [17], [36]), RL algorithms (Q-learning, SARSA, actor-critic, etc [12], [37]–[41]), and deep reinforcement learning (DRL) approaches [37]–[39], which is a combination of neural network and RL algorithms for BS switch off/on have been proposed. There are also hybrid methods that combine both heuristic approaches and machine learning approaches for finding the optimal BS switch-off/on strategy [17], [36], [42], [43].

Among the machine learning techniques, RL easily lends itself to solving the BS switching problem because it can learn

the best action to take in a given environment or scenario through a feedback reward system. Several works on BS switch off/on have been implemented using the RL in the literature. For example, in [37]–[39], Q-learning frameworks for BS switching and traffic offloading in a heterogeneous network were proposed. In these works, the heterogeneous networks comprise an MBS and several SBSs, and the learning takes place at the MBS, which serves as the controller of all the BSs under its coverage. The drawback of Q-learning algorithms is that since the process of Q-learning involves the use of tables (Q-tables) to store the learnt state-action values (Q-values), in situations where a large number of actions needs to be learnt, it would take very long for the Q-table to converge. In addition, an extensive memory would be required to store the learnt Q-table, and as a result, with increasing actions or states, the generalization ability of Q-learning begins to diminish [44]. Hence, the tabular approaches of RL (Q-learning and state-action-reward-state-action (SARSA) algorithms) are only feasible when the network dimension is small or medium. However, when the network dimension becomes very large, as obtained in ultra-dense 5G and beyond networks, the computational burden required to learn the Q-table dramatically increases due to a large number of states or actions involved.

To overcome the curse of dimensionality challenge of conventional Q-learning and SARSA algorithms due to tabular learning techniques, function approximators have been employed, which could be mathematical functions or deep learning algorithms. In this regard, the work in [16] extended the works in [37], [38] by proposing SARSA with value function approximation to enhance the scalability and generalization ability of the conventional SARSA algorithm so that it can be applied to large-scale networks. Similar attempts to improve the scalability of Q-learning models were carried out in [45]–[47] where deep-Q networks, double-deep Q-networks RL were employed. Generally, deep-Q networks can handle continuous states and action spaces, but their performance degrades when a huge discrete action space is considered [44].

Actor critic [48], [49] and deep-actor-critic [50], [51] RL have also been employed for BS switching. The conventional actor-critic algorithm is unsuitable for application in problems involving large state or action spaces because the critic employs a state action value table as its value function, requiring ample storage for large-scale problems [50]. Similarly, in a conventional deep actor-critic algorithm, the output of the actor-network is a probability distribution of possible actions and is only feasible when a few numbers of action spaces are considered. In the BS switching problem, the number of action spaces would be huge (since the number of action spaces increases exponentially with the number of SBSs), especially when ultra-dense deployment is considered [52], [53]. Hence, the proposed actor-critic and deep actor-critic solutions are only suitable for small to medium-scale network deployments, and there is still the need for a scalable solution that is adaptable to any network size to be developed.

Therefore, in this work, we develop a solution that is able to overcome the challenges of handling large state and action spaces as well as huge discrete action spaces facing both

conventional actor-critic and actor-critic DRL. Specifically, we leverage federated learning alongside actor-critic RL algorithm to develop a secure energy-saving framework for ultra-dense 5G and beyond cellular networks known as federated assisted modified actor-critic (FAMAC). FAMAC is able to learn the optimal SBS switch-off/on policy even when the number of SBSs in the network becomes very large while incurring minimal signaling overhead compare to other state-of-the-art solutions. The proposed model is trained in an offline manner, after which the trained model is implemented in real-time for energy saving in the network.

A. Contributions

This work proposes a federated-assisted modified actor-critic (FAMAC) RL framework for secured energy saving in ultra-dense 5G and beyond networks while satisfying the QoS constraints of the network. The following are the main contributions of this work:

- We employ federated learning to develop traffic prediction model based on a real network dataset to preserve the privacy of user traffic while minimizing the signalling overhead incurred during the process of learning the BS switching strategy due to information exchange between SBSs and the MBS.
- We present the mathematical model for computing the power consumption of the ultra-dense network and formulate the SBS switching problem as a constrained combinatorial optimization problem.
- We develop a modified actor-critic framework to determine the optimal switch-off/on pattern of the SBSs in the network while respecting the QoS constraints. Unlike conventional actor-critic algorithm, we developed a set of procedures that would enable the proposed framework to overcome the limitations of conventional actor-critic algorithms in handling combinatorial problems with large discrete action space and multiple constraints.
- We develop benchmark models comprising both heuristic and machine learning models for the purpose of comparing the performance of the proposed model.
- We carry out extensive simulations using a dataset obtained from a real network in order to evaluate the performance of the proposed framework.

III. SYSTEM MODEL

A. Network Model

An ultra-dense heterogeneous network (UHDN) consisting of several macro cells (MCs) is considered where each MC comprises a MBS, and several SBSs (remote radio head (RRH), micro, pico and femto) having varying capacities and power consumption profiles. The architecture considered for the UHDN is the separated control and data architecture where the MBSs function as control BSs for the purpose of signalling, low data rate transmission, and activation and deactivation of the SBSs deployed in their coverage. The SBSs function as data BSs and are deployed in hotspot areas for the purpose of capacity and throughput enhancement. In addition, vertical traffic offloading is employed whereby the traffic load

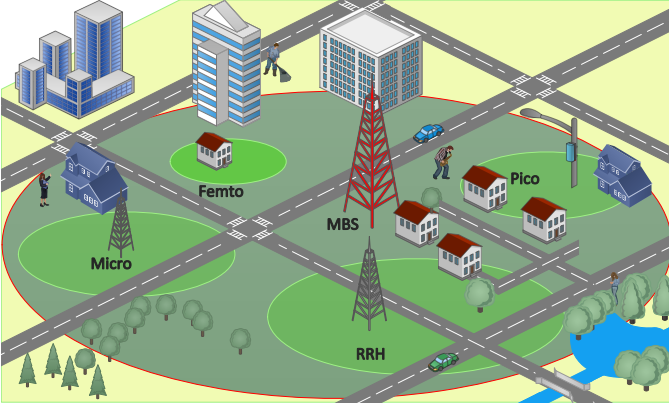


Fig. 1. An ultra-dense network comprising three macro cells with each consisting of an MBS and four types of SBSs (RRH, micro, pico and femto BS).

of under-utilized SBSs can be transferred to the MBS, and the under-utilized SBSs switched off in order to minimize the energy consumption of the network. The goal of traffic offloading is to ensure that the traffic demand of the users connected initially to the SBSs turned off is served by the MBS to maintain the QoS of the network.

It is assumed in this work that prior to the BS switch off/on operation, the network is able to serve the traffic demand of all the users associated with the network, which implies that the UDN has sufficient radio resources to serve all user demands when all the BSs in the network are active. However, this cannot be guaranteed when the BS switch-off/on scheme is implemented since the number of radio resources in the network will reduce when some SBSs are switched to save energy. Hence, the QoS in this work is described as the capacity of the network to serve the traffic demands of all users following the implementation of the proposed BS switch-off/on mechanism. This metric for quantifying the QoS has been referred to as coverage loss in [54]. The network model this work considers is illustrated in Fig. 1. It should be noted that since the separated architecture is considered in this work, it is assumed that all the MCs have similar deployment characteristics in terms of the composition of SBS (i.e., all have the same type of SBSs, RRH, micro, pico and femto) except that the number of each type of SBSs may vary from one MC to another. In addition, the MCs are assumed to function in a decentralized manner such that the MBS in each MC is saddled with the responsibility of controlling the activities of the SBSs in its coverage.

B. Base Station Load

The resources of a BS are normally segmented into units known as resource blocks (RBs). For a given user x that is associated with a particular BS j , the transmission rate can be expressed as:

$$\sigma_{x,j} = \zeta_x \kappa_{RB} \log_2(1 + \gamma_{x,j}) \quad (1)$$

where ζ_x is the number of RBs assigned to user x by BS j , κ_{RB} is the bandwidth of one RB, and $\gamma_{x,j}$ is the signal-to-noise-plus-interference-ratio received by user x from BS j .

In order to meet the QoS requirement of each user, a certain amount of frequency is assigned by the network to each user. Hence, it is necessary to determine the minimum number of RBs that is required to meet the minimum data rate (Φ_x) of the user in order to guarantee that its QoS is satisfied by the network. As a result, the number of RBs $N_{x,j}$ that must be assigned to user x by BS j is given by:

$$N_{x,j} = \frac{\Phi_x}{\kappa_{RB} \log_2(1 + \gamma_{x,j})} \quad (2)$$

The BS load can therefore be defined as the ratio of the number of RBs required to serve the traffic demand of all the users associated with a BS to the total number of RBs that is available in the BS [39]. This can be expressed as:

$$\psi_j = \frac{\sum_{v=1}^{\Lambda} N_{x,j}}{M_x} \quad (3)$$

where Λ is the number of users connected to BS j and M_x is the total number of RBs in BS j .

C. Power Consumption of Ultra-Dense Heterogeneous Networks

The total power consumption of the UDN is made up of the power consumption of the several MCs in the network each comprising a MBSs and a number of SBSs. According to the Energy Aware Radio and neTwork technologies (EARTH) model [55], [56], the instantaneous power consumption of a BS P_{BS} can be expressed as:

$$P_{BS} = \begin{cases} P_o + \mu P_{tx} & 0 < P_{tx} < 1 \\ P_s & P_{tx} = 0, \end{cases} \quad (4)$$

where P_o and P_s are the constant and sleep power consumption component, respectively, μ denotes the power amplifier (PA) efficiency, and P_{tx} is the transmit power which can be expressed as:

$$P_{tx} = \begin{cases} \psi P_{\max} & 0 < \psi < 1 \\ P_{\max} & \psi = 1, \end{cases} \quad (5)$$

We consider all SBSs of the same type to have similar hardware, such that μ and P_o are the same. We do not consider power allocation, as a result, we assume that the transmit power of each type of BS is fixed and constant among BS belonging to the same category.

Combining (4) and (5), the total instantaneous power consumption $P_{\beta,t}$ of a BS at time t can be expressed as:

$$P_{\beta,t}(\psi_t) = P_o + \psi_t \mu P_{\max}, \quad (6)$$

The value of P_o , μ , and P_{\max} depends on the type of BS (i.e., MBS, RRH, micro, pico and femto BS).

Therefore, the total instantaneous power consumption of an ultra-dense 5G and beyond cellular network P_{total} with several MCs (indexed with i) and different types of SBSs (indexed with j), at the time, t can be expressed as:

$$P_{\text{total}}(\psi_t^{i,j}) = \sum_{i=1}^{N_m} \sum_{j=1}^{N_b} P_{\beta,t}^{i,j}(\psi_t^{i,j}), \quad (7)$$

where $P_t^{i,1}$ represents the power consumption of the MBS in the i^{th} MC.

IV. PROBLEM FORMULATION AND OPTIMIZATION OBJECTIVE

A. Problem Formulation

A certain interval of time (T) is considered such that T is subdivided into various time slots (in mins) which are of the same duration L (in mins). We also define an index vector u which is used to store all the time slots in successive order and is given as $\nu = [1, 2, \dots, N_T]$, where N_T denotes the number of time slots and is given by $N_T = T/L$. We represent the BSs in each MC by $\beta^{i,j}$ where $\beta^{i,1}$ is used to identify the MBS. The scenario considered in this work is one where the UDHN can decide to turn off/on a certain number of SBSs when the traffic load of the network is low to reduce the amount of energy consumption in the network. We aim to determine the optimal switching policy (i.e., the optimal combination of SBSs to switch off/on) at each time slot that would give the maximum amount of energy saving in the UDHN.

Hence, the total power consumption of the UDHN (accumulated over all the time slots) that would be obtained with the implementation of BS switch off/on can be expressed as:

$$P_{\text{total}}(\psi_t^{i,j}, \Gamma_t^{i,j}) = \sum_{\nu=1}^{N_T} \sum_{i=1}^{N_m} \sum_{j=1}^{N_b} [\Gamma_t^{i,j} P_{\beta^{i,j}}^{i,j}(\psi_t^{i,j}) + (1 - \Gamma_t^{i,j}) P_s^{i,j}], \quad (8)$$

where $P_s^{i,j}$ represents the power consumption of the BS when they are turned off or operated in low power consumption mode. (i.e., sleep mode power consumption) and $\Gamma_t^{i,j}$ denotes the off/on state of the j^{th} BS in the i^{th} MC at time t i.e.,

$$\Gamma_t^{i,j} = \begin{cases} 1, & \text{if } \beta^{i,j} \text{ is on} \\ 0, & \text{if } \beta^{i,j} \text{ is off} \end{cases} \quad (9)$$

Since the MBS is always active, $\Gamma_t^{i,1} = 1, \forall t$.

B. Optimization Objective

The optimization objective is to minimize the total power consumption of the UDHN while satisfying the QoS requirement of the network. Therefore, the power minimization objective function can be defined as:

$$\min_{\Gamma_t^{i,j}} P_{\text{total}}(\psi^{i,j}, \Gamma_t^{i,j}) \quad (10)$$

$$\text{s.t. } \Phi^i = \chi^i, \quad \forall i, j, \quad (11)$$

$$\hat{\psi}^{i,1} \leq \psi_m^{i,1}, \quad \forall i, \quad (12)$$

$$\Gamma_t^{i,j} \in \{0, 1\}, \quad \forall i, j. \quad (13)$$

We provide an explanation for the constraints in (10) in the following. The total traffic demand of the MC, Φ^i , when all the BSs in the MC i are turned on (i.e., prior to traffic offloading) is expressed as,

$$\Phi^i = \sum_{j=1}^{N_b} \psi^{i,j}, \quad \forall i. \quad (14)$$

To satisfy the QoS requirement, we try to ensure that the traffic demand of any SBS that is switched off will be offloaded to the MBS, hence, the actual traffic load of MBS during the

process of traffic offloading which is denoted by $\hat{\psi}^{i,1}$ can be expressed as,

$$\hat{\psi}^{i,1} = \psi^{i,1} + \sum_{j=2}^{N_b} \psi^{i,j} (1 - \Gamma_t^{i,j}), \quad \forall i. \quad (15)$$

When traffic offloading is completed, the traffic demand of the MC, χ^i can be expressed as,

$$\chi^i = \hat{\psi}^{i,1} + \sum_{j=2}^{N_b} \psi^{i,j} \Gamma_t^{i,j}, \quad \forall i. \quad (16)$$

Therefore, to satisfy the constraint in (11), which is the QoS requirement considered in this work, (14) must be equal to (16). We initially assumed that MBS will be capable of handling the traffic demand of all SBSs that are turned off. However, that might not always be the case, as there is a maximum limit to the amount of traffic demand that can be accommodated by the MBS, due to the amount of radio resources available at the MBS. As a result, we also need to introduce another constraint to cater to this situation by specifying the maximum traffic demand that can be served by the MBS in any time slot t as $\psi_m^{i,1}$. Therefore, the additional constraint is defined in (12). It should be noted that for the purpose of clarity, the key notations that have been in the work are summarized in Table I.

V. PROPOSED METHODOLOGY

The implementation procedure for the proposed FAMAC framework for BS switching in 5G and beyond networks comprises two stages. The first stage is the traffic prediction stage, where a federated learning model is developed to equip the MBS with a global knowledge of the traffic load of all the SBSs under its coverage. The second stage is the BS-switching stage, where a modified actor-critic DRL is developed to determine the optimal switching policy of the UDHN that would result in maximum energy saving in the network while maintaining the QoS of the network.

A. Traffic Prediction Stage

In the traffic prediction stage, we employ federated machine learning to obtain the future traffic loads of all the SBSs in the network. The reason for using federated learning in this work is to equip the decision-making entity located at the MBS, where the proposed FAMAC is being implemented, with the global knowledge of the traffic condition of all the SBSs under its coverage in order to enable it to make the right switching decision. Since the BS switch off/on the decision is made at a central server located at the MBS, without traffic prediction, each SBS will have to periodically send the information about its traffic condition to this server, which would result in increased signaling overhead, latency, and additional energy consumption due to repeated transfer of data to the MBS. Moreover, during the process of data transfer, the privacy of the user data can also be comprised by a third party. Hence, we have leveraged federated learning because only the encrypted version of the local weights of each model learned at each SBS is shared with the server in order to equip the MBS with

knowledge of the traffic condition of all SBSs at each time instance. Federated learning is essential because it ensures data privacy, as model training does not involve local data sharing. It also minimizes signalling overhead as the SBSs do not need to repeatedly send traffic information to the MBS for making BS switching decisions.

A brief description of the proposed federated learning-based traffic prediction model and the procedure for implementing the model is detailed in the following paragraphs.

1) *Federated learning-based traffic prediction model*: Federated learning is a machine learning technique that enables models to be trained collaboratively across multiple devices or network entities in different locations without sharing their data. In other words, in federated learning, the data used for training the model on individual devices is retained locally. It is only the updates to the parameters of the local models that occur during the training process that are shared with the central learning entity, which aggregates all the updates to obtain a global model. The global model is then shared with the individual devices, and this process is repeated until convergence or the expected performance is attained. The procedure for implementing federated learning is discussed in the following paragraphs [57], [58].

We consider an MBS that is equipped with a server and J SBSs which serve as its clients. Each SBS j would utilize its training data set φ_j with φ_j samples. Where the dataset, φ_j is defined as $\varphi_j = \{x_{j,v}, y_{j,v}\}_{i=1}^{\varphi_j^k}$, $x_{j,v}$ denotes the neural network input of client j and $y_{j,v}$ is the corresponding target. The main objective of the federated learning process is to minimize a loss function which can be defined as [59]:

$$\min_{\omega \in \mathbb{R}^n} F(\omega) \equiv \frac{1}{\varphi} \sum_{j=1}^J \varphi_j F_j(\omega), \quad (17)$$

where $F_j(\omega)$ is the loss function of each client j (local loss function), $\omega \in \mathbb{R}^n$ is a vector of the parameters of the local model with dimension n , and $\varphi = \sum_{j=1}^J \varphi_j$ is the sum of all the client's data samples.

The step-by-step procedure for the implementation of FL is itemized below [60]:

- 1) The central entity shares the global model parameters with the J clients participating in collaborative learning.
- 2) The gradient that is required to minimize the local loss function is calculated by each client $j \in J$ using their local dataset.

$$\theta_j[t] = \nabla_{\omega} F_j(\omega[t], L_j), \quad (18)$$

where t denotes the communication round, and $\theta_j[t]$ is the local gradient of each client, j .

- 3) After exposure to each batch size, the local model weights are updated according to the following:

$$\omega_j[t+1] = \omega_j[t] - \alpha \theta_j[t], \quad (19)$$

where the learning rate is denoted by α .

- 4) Then, rather than transmitting the local data from each client to the central entity, the weights of the local models are sent over the wireless link.

- 5) Upon receipt of the weights from all clients, the central entity then aggregates the weights by computing their average as follows [61]:

$$\omega_j[t] := \frac{1}{\sum_{j=1}^J \varphi_j} \sum_{j=1}^J \varphi_j \omega_j[t] \quad (20)$$

Then, the average weights obtained from the global model are sent back to all participating clients to be used to update the weights of their local models.

The communication rounds continue until the global model converges. This global model is then used to predict the future traffic load of the SBSs in the network. Because the future traffic prediction of the SBS traffic load is a time series prediction, only the historical traffic load of each SBS is needed as input to the global model in order to obtain the future traffic that is needed to be fed as input to the BS switching stage. The federated learning model in this work is developed using bi-directional long and short-term model (LSTM), and in the following paragraphs, we briefly discuss the bi-directional LSTM model.

The bi-directional LSTM is an enhanced implementation of the traditional LSTM model. The conventional LSTM was introduced to handle the problem of vanishing and exploding gradient that affects the performance of conventional recurrent neural networks (RNNs), thereby preventing them from learning long-term dependencies between data samples. Thus, LSTM is able to overcome the problem of unstable gradients by enhancing the gradient flow. This is achieved by the introduction of memory and three gates (forget, input, and output gates) in the LSTM architecture. These gates serve as filters that regulate the way information moves from the input to the out of the cell during the process of predicting the output sequence, thereby improving the overall performance of LSTM compared to RNNs [62]. The Bi-directional LSTM also improves on the performance of the traditional LSTM by capturing the dependencies between past and future time steps, which make them more suitable for sequence predictions such as time series forecasting, speech recognition, etc. It is able to achieve better performance than the traditional LSTM because it combines two traditional LSTM models with the first processing information in the forward direction while the other in the backward direction, and the final output is obtained by concatenating the output from both LSTM models [63]. The pseudocode for the proposed federated-based traffic prediction model is presented in Algorithm 1.

B. BS Switching Stage

In the BS-switching stage, the future traffic loads of the network that was obtained from the traffic prediction stage are fed into the modified actor-critic model to determine the optimal policy in terms of the set of SBSs that should be turned off per time in order to minimize the overall energy consumption of the network. In the following paragraphs, we present an overview of conventional actor-critic RL, followed by the proposed modified actor-critic model alongside its implementation procedure.

Algorithm 1 Federated Algorithm For Traffic Prediction

```

1: Require: Local Dataset  $D_n$ , Number of BS  $N$ ,
   Number of federated rounds  $T$ ,
   Number of local Iteration  $e$ ,
   Learning rate  $\eta$ 
2: Initialize global weights  $\Omega^0$ 
3: for  $t = 1$  to  $T$  do
4:    $j = \sum_{n \in N} |D^n|$ 
5:   for  $n \in N$  in parallel do
6:     Send the global model  $\Omega^t$  to SBS $_n$ 
7:      $\Delta\omega_n^t \leftarrow \text{LOCALTRAINING}(n, \Omega^t)$ 
8:   end for
9:    $\Delta W \leftarrow \sum_{n \in N} \frac{|D^n|}{j} \Delta\omega_n^t$ 
10:   $\Omega^{t+1} \leftarrow \Omega^t - \eta \Delta W$ 
11: end for
12: Global model  $\Omega^T$  for traffic prediction.
13: function LOCALTRAINING( $n, \Omega^t$ )
14:   $\omega_n^t = \Omega^t$ 
15:  for  $k = 1$  to  $e$  do
16:    for each batch  $\mathbf{b} = \{\mathbf{x}, \mathbf{y}\}$  of  $D^i$  do
17:       $\omega_n^t \leftarrow \omega_n^t - \eta \nabla L(\omega_n^t; \mathbf{b})$ 
18:       $s.t. L(\omega; \mathbf{b}) = \sum_{(x,y) \in \mathbf{b}} l(\omega; x; y)$ 
19:    end for
20:  end for
21:   $\Delta\omega_n^t \leftarrow \omega_n^t - \omega_n^t$ 
22:  return  $\Delta\omega_n^t$  to the MBS
23: end function

```

1) *Conventional Actor-Critic Deep Reinforcement Learning*: The principle of DRL involves being able to train an agent to take optimal actions in an unknown environment by exposing the agent to the environment and using feedback obtained from previous and current actions taken to optimize future action. During each time instance t , the agent observes the current state s_t , then takes an action a_t according to a given policy, $\pi(a_t|s_t)$. The agent will obtain a reward r_t , which is fed back to the agent. Then, the policy governing the behaviour of the agent is updated according to the feedback obtained. This process is repeated until the agent learns to take the correct action at every given time instance. Actor critic is a class of RL algorithms where the agent comprises two parts, an actor and a critic. On one hand, the actor's function is to take actions while following a policy $\pi(a_t|s_t)$, where $\pi(a_t|s_t)$ is known as the conditional probability density function. The function of the critic on the hand is to evaluate the decisions taken by the actor using a Q -value which can be expressed as:

$$Q^\pi(s_t, a_t) = \mathbb{E}_{a_t \sim \pi(a_t|s_t)} [R_t | s_t, a_t] \quad (21)$$

where $\mathbb{E}[R_t | s_t, a_t]$ denotes a conditional expectation with respect to the policy $\pi(s_t | a_t)$, R_t represents the cumulative discounted reward and is given by:

$$R_t = \sum_{t'=t}^{\infty} \gamma^{t'-t} r_{t'}, \quad \gamma \in [0, 1] \quad (22)$$

where γ is the discount factor. However, due to the difficulty involved in obtaining an explicit expression of $\pi(s_t | a_t)$, deep neural networks are employed as parameterized function approximators to estimate $\pi(s_t | a_t)$ and $Q^\pi(s_t, a_t)$ in DRL. The parameter vectors for the actor and critic are represented with Θ_t and ω_t and $\pi(s_t | a_t; \Theta_t)$ and $Q^\pi(s_t, a_t; \omega_t)$ are their corresponding parameterized functions, respectively. The agent aims to minimize the actor's loss function $-J(\Theta_t)$ and can be defined as:

$$-J(\theta_t) = -\mathbb{E} [Q^\theta(s_t, a_t; \omega_t)] \quad (23)$$

According to [44], [53], the gradient of $J(\Theta_t)$ can be obtained by:

$$\nabla_\theta J(\theta_t) = \mathbb{E} [\nabla_\theta \log \pi(a_t | s_t; \theta_t) Q^\theta(s_t, a_t; \omega_t)] \quad (24)$$

The rule for updating θ_t can obtained using gradient descent as follows:

$$\theta_{t+1} = \theta_t - \alpha_a \cdot (-\nabla_\theta J(\theta_t)) \quad (25)$$

where the learning rate of the actor is denoted by α_a .

The parameter vector of the critic ω_t is updated based on temporal-difference (TD) learning [44]. In TD learning, the critic's loss function $C_Q(\omega_t)$ can be defined as the expectation of the square of the TD error $\delta_Q(\omega_t)$ and can be expressed as:

$$C_Q(\omega_t) = \mathbb{E} [(\delta_Q(\omega_t))^2] \quad (26)$$

where $\delta_Q(\omega_t)$ the represents the difference between the estimated Q -value and the TD target and can be expressed as:

$$\delta_Q(\omega_t) = r_t + \gamma Q^\theta(s_{t+1}, a_{t+1}; \omega_t) - Q^\theta(s_t, a_t; \omega_t), \quad (27)$$

where $r_t + \gamma Q^\theta(s_{t+1}, a_{t+1}; \omega_t)$ depicts the TD target and $Q^\theta(s_t, a_t; \omega_t)$ the Q -value. The goal of the critic is to ensure that the loss function $C_Q(\omega_t)$ is minimized and this can be achieved using the update rule for ω_t that is derived from gradient descent as follows:

$$\omega_{t+1} = \omega_t - \alpha_c \nabla_\omega C_Q(\omega_t) \quad (28)$$

where α_c denotes the critic's learning rate.

There is often the challenge of large variance from the gradient $\nabla_\theta J(\theta_t)$ which occurs when trying to approximate $Q^\pi(s_t, a_t)$, thereby leading to poor convergence. Hence, the V -value has been introduced to overcome this problem [19], [64] and can be expressed as:

$$V^\pi(s_t) = \mathbb{E}_{a_t \sim \pi(a_t|s_t)} [R_t | s_t] \quad (29)$$

The approximation of $V^\pi(s_t)$ instead of $Q^\pi(s_t, a_t)$ can help to minimize the variance. Using the parameterized v -value $V^\theta(s_t; \omega_t)$, the TD can be expressed as:

$$\delta_V(\omega_t) = r_t + \gamma V^\theta(s_{t+1}; \omega_t) - V^\theta(s_t; \omega_t), \quad (30)$$

and the critic loss function can be expressed as:

$$C_V(\omega_t) = \mathbb{E} [(\delta_V(\omega_t))^2] \quad (31)$$

Moreover, $\delta_V(\omega_t)$ gives a balanced estimation of Q -value [64].

Hence, the gradient $\nabla_\theta J(\theta_t)$ in (24) can be rewritten as:

$$\begin{aligned} \nabla_\theta J(\theta_t) &= \mathbb{E} [\nabla_\theta \log(\pi(a_t | s_t; \theta_t)) Q^\pi(s_t, a_t)] \\ &= \mathbb{E} [\nabla_\theta \log(\pi(a_t | s_t; \theta_t)) \delta_V(\omega_t)] \end{aligned} \quad (32)$$

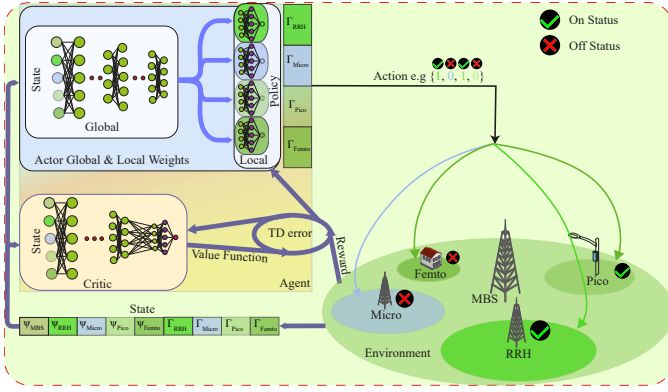


Fig. 2. The framework for implementing the modified actor-critic deep reinforcement learning algorithm.

2) Modified Actor-Critic Deep Reinforcement Learning:

The basic actor-critic DRL algorithm described in the preceding paragraphs is mostly suitable for decentralized implementation at different entities in the network. However, due to the combinatorial nature of the BS-switching problem considered, the switching action of the SBSs has to be learned together in a combined manner. As a result, the learning must be carried out in a centralized and co-ordinated manner. Hence, the conventional actor-critic DRL algorithm may not be suitable for this kind of problem for the following reasons: First, the actions taken by one SBS affects the other SBSs in the network as the BS switching problem is a combinatorial problem, so it is not possible to just implement a decentralized actor-critic DRL algorithm where each SBS serves as the agent as this would not result in learning a globally optimal solution that can minimize the overall energy consumption of the network. Second, to ensure that the QoS of the network is maintained, the actions taken by the SBSs also depend on the traffic condition of the MBS. Hence, to accommodate the dependencies of the actions of the SBSs and the need to satisfy the QoS of the network, there is a need to modify the conventional actor-critic DRL algorithm.

Unlike the conventional actor-critic algorithm, which is mainly suitable for decentralized multi-agent learning, the modified actor-critic DRL that is proposed in this work is a centralized multi-agent DRL system where the decision regarding the switching policy of all SBSs in the network is made in a central entity (in this case at the MBS) which is equipped with global information about the traffic conditions of the SBSs, that is needed to determine the best switching policy, from the future traffic load of the network that is obtained from the federated learning model. The major modification is with respect to the actor network. Usually, the output of the actor-network of a conventional actor-critic DRL algorithm is a probability distribution comprising all possible actions that can be taken. This output is only practicable when the number of possible actions is relatively small. However, in our work, the number of actions scales exponentially with the number of SBSs ($2^{(N_b-1)}$), which means that the actions space would be very huge since we are considering an ultra-dense BS deployment scenario. This will, in turn, require a very

large number of neurons at the output to be able to output the probability distribution. In addition, the huge action space may lead to inefficient exploration of the action space during the learning process, thereby degrading the overall performance of the algorithm.

To overcome the aforementioned challenges, we redesigned the actor network in such a way it can output a single deterministic action vector to represent the operating condition of each SBS in the network. To achieve this, we replaced the softmax function, which is responsible for generating the exponential action space, with a sigmoid function, so that the action of each SBS is represented by a sigmoid output. By so doing, we are able to reduce the exponential action space to a linear action space which improves the efficiency of exploration and dramatically enhances the overall performance of the proposed method. Therefore, in our modified approach, the actor learns the individual switching policies of the SBSs separately using the sigmoid function, after which the outputs from each sigmoid function are combined to give a combination of switching actions as the actor's output.

The modified actor Network is divided into two parts, first, the global actor network weights Θ , and the local actor network weights θ_n , where $n \in N_b$ is the number of SBS. The global weights are shared among all SBS actors during training. The shared weights are updated based on aggregated gradients, which allows the SBS policies to be coordinated. Since the switch-off action of one SBS affects the options of other SBSs, sharing global weights enables the joint action space to be explored efficiently. The local weights for each SBS actor are updated separately using only the local gradient for that SBS. These private weights allow each SBS to extract features unique to its traffic patterns and network environment. The local weights also help facilitate the learning process for individual SBS actors. In essence, the global weights promote cooperation between SBS switch-off policies, while the local weights capture specialized behaviour. This combination of shared and private parameters enables the actor-network to handle the large joint action space and learn coordinated yet personalized policies for BS switching.

The loss function of the conventional actor-critic DRL 23 is then modified to reflect the combination of sigmoid outputs for each SBS in the proposed solution. The equation 23 is modified by replacing the weight $\theta \rightarrow [\Theta^z \ \theta_n] \rightarrow \Theta^p$ and therefore the loss gradient of actor $\nabla_{\Theta} J(\Theta^p)$, where Θ^z is constant global weight connected to n-SBS, $n = p \in N_b$ is the number of SBS. Based on modification of 23, the actor gradient loss in 32 can now be written as:

$$\begin{aligned} \nabla_{\Theta^p} J(\Theta_t^p) &= \mathbb{E} [\nabla_{\Theta^p} \log(\pi(a_t | s_t; \Theta_t^p)) \delta_V(\omega_t)] \\ &\approx \frac{1}{T} \sum_{t=1}^T [\nabla_{\Theta^p} \log(\pi(a_t | s_t; \Theta_t^p)) \delta_V(\omega_t)] \end{aligned} \quad (33)$$

where $\nabla_{\Theta^p} J(\Theta_t^p)$ represents the gradient of the actor loss for an individual network of $n \in N_b$ SBS which contains global weight Θ^z and local weights θ_n , T is the number of collected transitions. In this work, we use TD(0), $\pi(a_t | s_t; \Theta_t^p)$ is the predicted probability of selecting action a_t given state s for

the t -th transition in the network n , $\delta_V(\omega_t)$ is the advantage value or TD for the i -th transition.

The update rule of Θ_p can be derived based on gradient descent. However, since we introduced the local and global weights for parameters of the actor network, the update is treated differently from the actor update equation 25. Each local weight is updated by extracting the local gradient weights θ_n from equation 33, and this portion of the weight is updated using the equation 25.

$$\theta_n = \theta_n + \alpha^\theta \cdot \nabla_{\theta_n} J(\theta_n) \quad (34)$$

For the global weight Θ^z connected to all n -local networks, the update procedure is to extract the weight from equation 33. Since the individual actor gradient loss is different for each n -SBS, the update is based on the aggregated gradients across all SBS actors. Then, the global weight is updated to have the average Θ as follows:

$$\Theta^z = \Theta^z + \alpha^\Theta \cdot \frac{1}{N} \sum_{n=1}^N \nabla_{\Theta^z} J(\Theta^z) \quad (35)$$

The critic network employed in this work is the same as that of the conventional actor-critic DRL.

3) *Problem Reformulation*: To apply MAC-RL, we reformulate the BS switching problem as an MDP with the MBS serving as the agent. The states, actions, and rewards (cost) are defined as follows:

a) *States*: The states of the MAC-RL comprises the traffic load of MBS and that of the SBSs under its coverage before BS switching and traffic offloading take place, as well as the current on/off status of the SBS. Thus, the state s_t can be defined as:

$$s_t = [\psi_t^{i,1}, \psi_t^{i,2}, \psi_t^{i,3}, \dots, \psi_t^{i,N_b}, \Gamma_t^{i,2}, \Gamma_t^{i,3}, \dots, \Gamma_t^{i,N_b}]. \quad (36)$$

The traffic loads of the BSs and the current on/off status of the SBSs are selected to be the states in this work because they are the main parameters whose variation significantly represents the environment and contribute to the computation of power consumption of the UDHN.

b) *Actions*: The actions of the proposed MAC-RL comprises switching off/on the different types of SBSs in the network. This is usually a binary decision where the status of the SBSs that are on is denoted with binary 1, while those that are turned off are represented with binary 0. Thus, the action a_t can be represented as:

$$a_t = \{\Gamma_t^{i,2}, \Gamma_t^{i,3}, \Gamma_t^{i,4}, \dots, \Gamma_t^{i,N_b}\} \\ = \{\Gamma_t^{i,j} | j \in \{2, \dots, N_b\}\}. \quad (37)$$

where $\Gamma_t^{i,j} \in \{0, 1\}$ is the on/off decision for the j^{th} SBS in the network. Therefore, the complete action vector a_t specifies the ON/OFF decision for each SBSs at time t . It should be noted that index j starts from 2 because the MBS is always kept on to offload the traffic load of the sleeping SBSs in order to ensure service continuity to the users originally associated with them.

c) *Reward*: In this work, we designed the reward so that the agent will explore different action combinations, and hence we set different rewards based on the condition of the network. Three reward levels are considered, considering the QoS requirements and switching options that the agent can perform. The first level of reward is set for the condition where the action of the agent violates the traffic offloading capacity of the MBS. For such a case, we penalize the agent to avoid taking that action. Moreover, we also set a small negative reward if the agent chooses not to switch off any BS. In addition, to allow smooth learning, the agent gets a positive reward when the energy saved exceeds 0. Nevertheless, we normalize the reward to avoid a large network update to allow the network to learn parameters smoothly. The normalizing factor for positive reward is the maximum energy saved that keeps updated every time t and is given by:

$$P_{\text{saved}}^t = P_{\text{total}}(\psi_t^{i,j}) - P_{\text{total}}(\psi_t^{i,j}, \Gamma_t^{i,j}) \quad (38)$$

where $P_{\text{total}}(\psi_t^{i,j})$ (7) is the total power consumption of the UDHN when all the SBS are switched on, and $P_{\text{total}}(\psi_t^{i,j}, \Gamma_t^{i,j})$ (8) is the total power consumption when a switching action is selected. Initially, the maximum power saved is set to 0, and at every time step t during training, when the power saved is greater than the previous maximum power saved, the maximum power saved is updated and set to the value of the new maximum power saved that is obtained. Mathematically, the maximum saved power can be expressed as:

$$P_{\text{saved}}^{\text{max}} = \max_{t \in \{1, 2, \dots, T * N\}} P_{\text{saved}}^t \quad (39)$$

where P_{max} is given as the largest power saved among all the episodes (N) and trajectory(T) ($T * N$). And the reward at each time step is given as

$$r_t = \begin{cases} -1, & (\psi_t^{i,1} + \sum_{\substack{\Gamma_t^{i,n} \\ \forall \Gamma_t^{i,n}=0}} \psi_t^{i,n}) > 1 | (P_{\text{saved}}^t < 0) \\ -0.1, & \text{if no SBS is switched off} \\ P_{\text{saved}}^t / P_{\text{saved}}^{\text{max}}, & P_{\text{saved}}^t > 0 \end{cases} \quad (40)$$

Algorithm 2 shows the pseudo code for implementing the modified actor-critic deep reinforcement learning algorithm to determine the optimal base station switch-off/on policy for energy optimization. At the beginning of the learning, the actor-network representing the policy is initialized with global shared weights Θ and local weights θ_j for each SBS j . This architecture allows the actor to handle large discrete action spaces. Also, the critic network estimating the state-value function is initialized with weights ψ . The critic approximates the Q-values. Then, for each episode, the environment state s is reset. This state comprises the predicted traffic loads from the federated learning stage and the current status of the SBSs. The done flag is set to False to run for the maximum time steps in the episode. Furthermore, For each timestep in the episode, the current state s is input to the actor-network. The actor selects an action a by aggregating the outputs from the global

Algorithm 2 Modified Actor-Critic (MAC)

Require: Learning rate Global Actor ($\alpha^\ominus \in (0, 1]$),
: Learning rate Local Actor ($\alpha^\theta = \alpha^\ominus, \in (0, 1]$)
: Critic Learning (α^ψ), discount factor (γ), $\forall \in (0, 1]$
: Number of episodes M , Number of small cells N
: Number of time steps per episode T

- 1: **Input:** Initialize the actor network $\pi(a|s, [\Theta : \theta_i] : \forall i \in N)$
Initialize the critic network $V(s, \psi)$
- 2: **for** $m = 1$ to M **do**
- 3: Reset the environment state s_t
- 4: done = False
- 5: **for** $t = 1$ to T **do**
- 6: Observe state s_t , and ($\forall i$ in N) action $a_{t_i} = \cup(\mu_{\Theta+\theta_i}(s_t))$, then $a_t = \cup a_{t_i} \forall i$ in N
- 7: Execute actions a_t in the environment and observe the next state s_{t+1} and reward r_{t+1}
- 8: Calculate $TD = r + \gamma V(s_{t+1}, \psi_t) - V(s_t, \psi_t)$
- 9: **Accumulate and Update Critic Network**
 $\partial\psi = \nabla_\psi(TD)^2$ Accumulate
 $\psi = \psi - \alpha^\psi \partial\psi$ Update
- 10: **Accumulate Actor Network**
- 11: **for** $i = 1$ to N **do**
 $\partial(\Theta_i + \theta_i) = \nabla_{(\Theta+\theta_i)} \log \pi_{(\Theta+\theta_i)}(s_t, a_{t_i})(TD)$
- 12: **end for**
- 13: **Update Global Actor Network**
 $\partial(\bar{\Theta}) = \frac{1}{N} \sum_{i=1}^N \partial(\Theta_i), \forall i \in N,$
 $\bar{\Theta} = \bar{\Theta} + \alpha^\ominus \partial(\bar{\Theta})$
- 14: **Update Local Actor Networks**
- 15: **for** $i = 1$ to N **do**
 $\theta_i = \theta_i + \alpha^\theta \partial(\theta_i)$
- 16: **end for**
- 17: Update the current state $s_t = s_{t+1}$
- 18: **end for**
- 19: **end for**

and local weights for each SBS j . The joint action vector a is executed in the environment. The environment returns the next state s' and rewards r (power consumption) for taking action a . Then, the critic network evaluates the action by computing the temporal difference (TD) error between the target Q-value and estimated Q-value from the weights ψ . The critic loss is computed as the mean squared TD error, after which the critic weights ψ are updated by gradient descent on the loss to minimize the TD error. Next, the actor weights are updated using the policy gradient calculated from the critic's TD errors. This follows the advantage actor-critic formulation, where the policy gradient is based on the advantages rather than raw rewards. The global weights $\bar{\Theta}$ are updated by aggregating across all SBS actors. This enables coordination. The local weights θ_i are updated for each SBS actor separately to capture specialized behavior. Then, the environment state is updated to begin the next timestep. The process continues until max timesteps per episode are reached. Multiple episodes are run until the algorithm converges to the optimal policy.

The essential advantage of the proposed approach is that introducing both global and local weights in the actor enables

effective exploration of a vast discrete joint action space. In addition, scaling to large state spaces is facilitated by deep neural network function approximators for the actor and critic. In summary, the modified actor-critic approach leverages a two-network structure to handle discrete actions, uses the critic's temporal difference errors to update the actor via policy gradient, and learns coordinated yet personalized switch-off policies using global and local weights, ultimately converging to optimize energy saving of the UDHN.

C. The Complete FAMAC Framework

The complete FAMAC framework is illustrated in Fig. 3 while the flow chart presenting the implementation procedure is presented in Fig 4. The procedure for implementing the proposed FAMAC BS switching framework involves 2 phases: offline and online. Each of the phases are briefly detailed in the following paragraphs:

- 1) **Offline Phase:** This is the phase where both the federated learning traffic prediction model and the modified actor-critic DRL are trained using the historical data from the network. The procedure of the offline training is discussed in the following:
 - Network Initialization: The first step is initializing the UDHN infrastructure. The MBS provides umbrella coverage and comprises several SBSs (SBSs) including RRHs, micro, pico, femto that are deployed in hotspots for capacity boosting.
 - Historical Data Collection: With the network established, historical traffic load data are collected over time and stored locally at each SBS. This raw data remains at each SBS and is not shared.
 - Federated Learning for Traffic Prediction: A federated learning model is developed using the historical data collected at each SBSs for distributed privacy-preserving traffic prediction. The aim is to provide the MBS with knowledge of expected traffic loads of the SBSs in its coverage without needing to acquire actual traffic data, which leads to significant communication overhead (Algorithm 1).
 - Modified Actor-Critic DRL Agent for BS Switching: a customized actor-critic DRL agent is developed using the historical data collected from the network to learn intelligent policies for dynamic BS switch-off that minimize network power consumption over time (Algorithm 2).
- 2) **Online Phase:** This is the stage where the proposed FAMAC is installed in the network to provide real-time BS switching operation using the traffic load predicted by the trained federated learning model. The procedure for the online implementation is as follows:
 - Real-time Traffic Prediction: For real-time operation, at each time step, the trained federated learning model provides the MBS with predicted traffic loads for the SBSs under its control based on current conditions.
 - Optimized BS Switching: The predicted traffic loads and the current on/off state of the SBSs are input

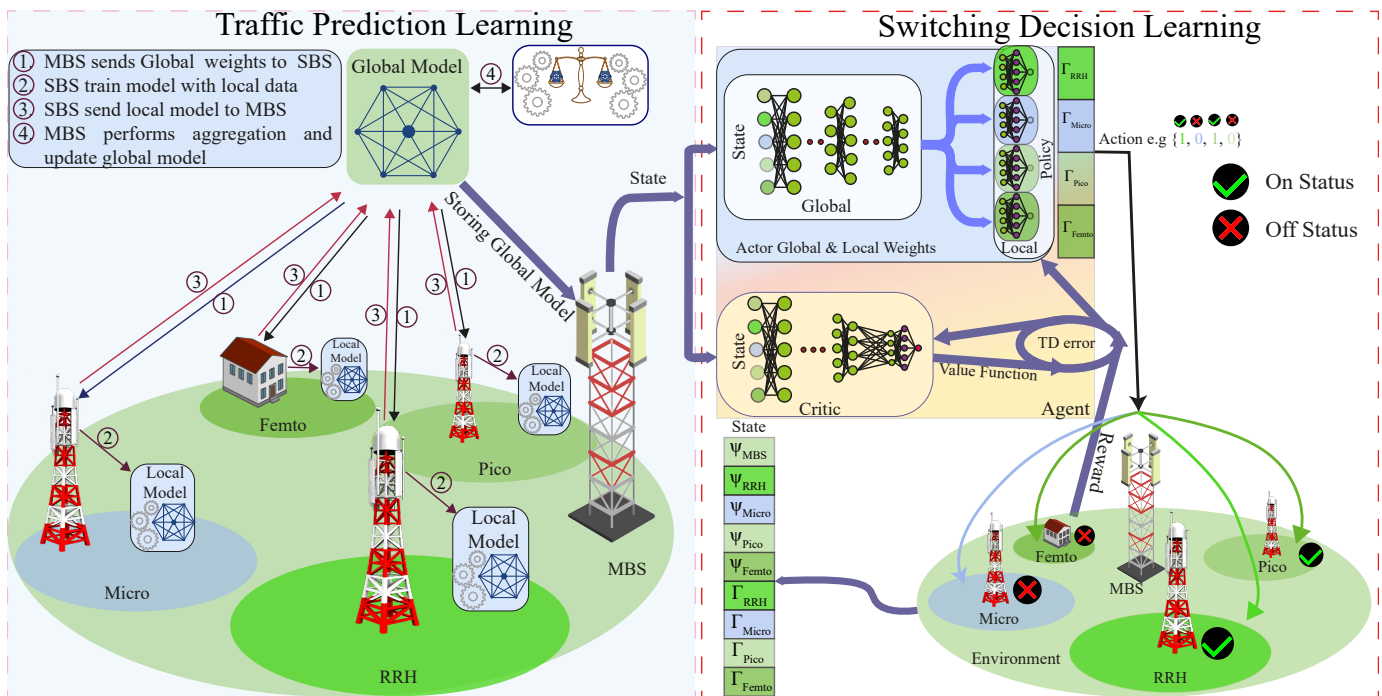


Fig. 3. The complete FAMAC framework comprising the federated-based traffic prediction and modified actor-critic deep reinforcement learning algorithm for BS switch off/on.

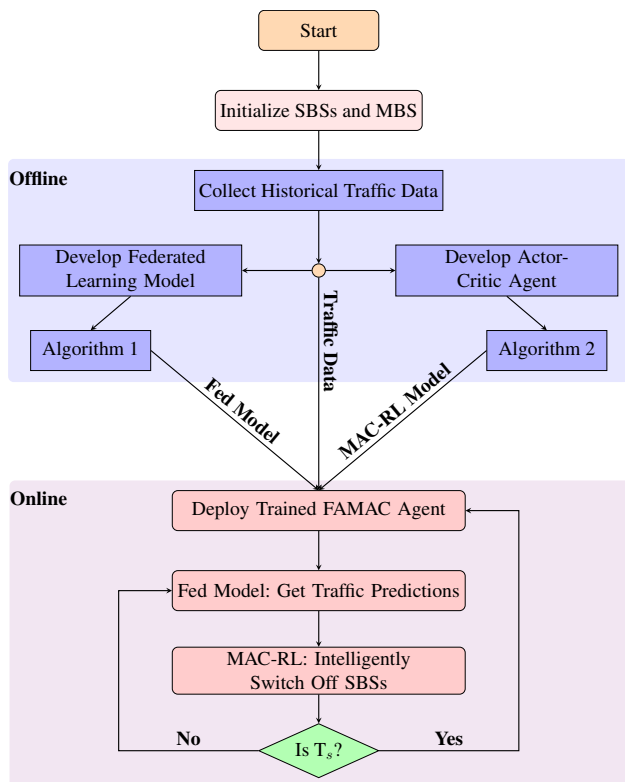


Fig. 4. The flowchart showing the implementation procedure of the proposed FAMAC BS switching framework.

as a state to the trained MAC DRL agent. Based on this, using its learned stochastic policy, the agent selects the optimal set of SBSs to switch off for the

current traffic.

- Execution: The joint switch-off actions are executed in the network environment, turning off the chosen SBSs.
- Continuous Adaptation: The principle of traffic prediction adopted when developing the federated learning model is a time series approach. This means that the previous traffic load of the network predicts the future traffic of the network. It is therefore essential to update the historical traffic database from which the future traffic load of the network is predicted by obtaining more recent data from the network within a given time interval T_s (where T_s could be once a day or a week, etc.). This would ensure that updated traffic predictions are obtained from the federated model and that the MAC DRL agent keeps adapting its BS switching strategy to the more updated SBS traffic predictions to optimize the energy saving of the network across changing conditions.

In a nutshell, FAMAC combines federated learning for distributed traffic prediction and a modified actor-critic reinforcement learning algorithm tailored for huge discrete action spaces to enable intelligent and secure data-driven optimization of BS switching for minimizing network power consumption across fluctuating traffic loads.

VI. PERFORMANCE EVALUATION

We evaluate the performance of the proposed BS switching framework using various metrics and compare its performance with those of other benchmark algorithms. It should be noted that since the UDHN is usually made up of many MCs,

TABLE II
POWER CONSUMPTION PARAMETERS FOR BSS [55]

Types of BS	Amplifier Efficiency (μ)	Power Consumption [W]		
		Transmit (P_{tx})	Fixed (P_o)	Sleep (P_s)
Macro	4.7	20	130	75
RRH	2.8	20	84	56
Micro	2.6	6.3	56	39
Pico	4.0	0.13	6.8	4.3
Femto	8.0	0.05	4.8	2.9

with each MC comprising one MBS which provides umbrella coverage and several types of SBSs, the proposed framework is designed in such a way that it would be implemented at each MBS. Hence, the MBS as saddled with the responsibility of controlling the operation of all SBSs under its coverage. Therefore, the proposed FAMAC model needs to be trained for only one MC in the UDHN, after which the trained model can be implemented in all the other MCs throughout the network. The power consumption parameters of the different types of BSs deployed in the UDHN are presented in Table II, while the parameters used in the simulation of the federated learning model and modified actor-critic model are presented in Table III.

A. Dataset and Pre-Processing

The traffic load of the MBS and the SBSs are needed to calculate the total power consumption of the UDHN using (8). To obtain information about the traffic load of the network, a dataset comprising the call detail record (CDR) of the city of Milan [65] was utilized during the simulation. Milan was partitioned into 10,000 square-shaped grids in the data set, each with a dimension of 235×235 meters. The CDR comprises calls, text messages, and internet activities carried out in each grid every 10 minutes for two months (November-December 2013). Although the activity levels contained in the data set are without units and the information about how the data was processed is not provided, the CDR of each grid is assumed to be the traffic load in this work since they represent the volume of network resources utilized by the users within each grid for each time slot. However, only the internet activity levels were considered as the traffic load for the BSs when processing the data because we are particularly interested in investigating 5G networks which is internet protocol (IP) based. Furthermore, to obtain the traffic load of an MBS, we combined the internet activity level of two randomly selected grids. In contrast, the internet activity of a single grid was considered to be the traffic load of each SBS. Finally, we normalized the traffic loads of each BS with respect to the total amount of radio resources in each type of the BS in the UDHN (i.e. macro, RRH, micro, pico and femto BSs). For the federated learning model development, the traffic load of 31 days, with each day comprising 144 samples, was obtained from the Milan dataset. This means that the total number of samples in the dataset for 31 days is 4464. 60% of the total samples is used for training (2680 samples), 20% of the dataset is used for validation (892 samples), and 20% of the total samples is used for testing (892 samples).

TABLE III
SIMULATION PARAMETERS

Parameter	Value
General	
Number of time slots	144
Number of days	1
Number of grids per MBS	2
Number of grids per SBS	1
Bandwidth of MBS	20 MHz
Bandwidth of RRH, Micro, Pico, Femto	15, 10, 5, 3 (MHz)
Traffic Prediction LSTM	
Dropout, Window Size	0.2, 59
LSTM Layers, Units, Bidirectional LSTM	3, window size, Enabled
Dense Units, Activation, Batch Size	1, Linear, 16
Loss Function,	Root Mean Squared Error
Optimizer, Epoch	Adam, 100
Modified Actor-Critic	
Optimizer/learning rate	Adam (0.01)
Global layers Actor	{32, 64, 128, 256}
Local layers Actor	{128, 64, 32}
Output layers Actor	$(N_b - 1)$ - sigmoids
Critic layers	{32, 64, 128, 256, 512, 32}
Output Critic layer	linear
Exploration rate	0.01
Discount Factor	0.90

B. Benchmarks

- **All-Always-ON (AAO):** In this approach, no BS switching is implemented, which means that all the BSs are constantly kept on. As a result, no traffic offloading occurs since none of the SBSs is switched off. In this approach, the QoS of the network is always maintained even though no energy saving is obtained as all the SBSs remain constantly on.
- **Exhaustive Search (ES):** This method is always guaranteed to find the optimal switching policy as it searches through all the possible switching combinations to determine the set of SBSs to switch off in each time slot. This method also ensures that the QoS of the network is always satisfied by considering the constraint (12) when determining the optimal switching policy. Hence, the goal of any BS-switching algorithm is to closely approximate the performance of the ES algorithm as much as possible.
- **Multi-Level Clustering (MLC):** The MLC approach is a clustering-based BS switching framework based on the K -Means algorithm. The MLC algorithm repeatedly clusters the SBSs deployed in the coverage area of the MBS according to their traffic load and tries to offload the cluster(S) of SBSs with the least traffic load to the MBS. Then, the total power consumption of the network when the traffic load of the cluster(s) is offloaded to the MBS is calculated. Finally, the cluster that gives the minimum power consumption in the UDHN is selected as the optimum cluster.
- **Threshold-based Hybrid cELL Switching Scheme (THESIS):** THESIS is an improvement on the MLC algorithm. It is a threshold-based hybrid algorithm comprising K -means clustering and an ES algorithm. In THESIS, the SBSs within the coverage of an MBS are clustered based on their traffic loads. After each clustering, the number of SBSs in each cluster is

compared to the threshold value, and then ES is applied to the clusters whose number of SBSs is less than the threshold value to determine the set of SBSs to switch off that would result in minimum energy consumption in the network. The clusters whose number of SBSs is greater than the threshold value are re-clustered so that their number of SBSs becomes smaller than the threshold value, and the ES algorithm is applied to each cluster. Then, the sets of SBSs that can be switched off in each cluster that would lead to minimum power consumption in the network while maintaining the QoS constraint are determined. Finally, the minimum energy consumption values obtained from the sets of SBSs that were switched off after each clustering and ES application are ranked in ascending order, and the one with the lowest power consumption is taken as the optimal set of SBSs to be switched off.

C. Performance Metrics

- **Root Mean Square Error (RMSE):** The RMSE is the cost function employed to evaluate the error of the bi-directional LSTM model. It depicts the discrepancy between predicted and actual values using Euclidean distance and can be expressed as:

$$RMSE = \sqrt{\frac{\sum_{i=1}^n (\hat{y}_i - y_i)^2}{n}} \quad (41)$$

where n denotes the average number of samples, y represents the target value, and y' is the predicted value.

- **Power Consumption:** This is the instantaneous power consumption of the network (in Watts) for the proposed and benchmark approaches that are obtained during simulations using (8), respectively. This metric is critical as it enables us to study the relative performance of each method in terms of how their instantaneous power consumption changes at different times of the day.
- **Energy Saved:** This metric quantifies the total amount of energy (in Joules) saved in the network when the proposed and benchmark methods are applied for a given duration. The energy saved is defined as the difference between the energy consumption when no switching algorithm is applied (when all BSs are on (i.e., E_{AAO})) and the energy consumption (E_{FAMAC} , E_{ES} , $E_{THEISIS}$, E_{MLC}) when a BS switching algorithm (FAMAC, THEISIS, MLC, ES) is applied. The energy saved E_s can be expressed as:

$$E_s = E_{AAO} - E_\theta \quad (42)$$

where $E_\theta \in \{E_{FAMAC}, E_{ES}, E_{THEISIS}, E_{MLC}\}$ and the total energy consumption for a whole day can be evaluated as:

$$E = \sum_{u=1}^{M_T} P_{\text{total}}(\psi_t^{i,j}, \Gamma_t^{i,j}) \times \kappa \times u \quad (43)$$

where $P_{\text{total}}(\psi_t^{i,j}, \Gamma_t^{i,j})$ is the power consumption (W) of the UDHN at a given time slot u . Since u is considered to be 10-minutes in the dataset, a whole day (24 hours)

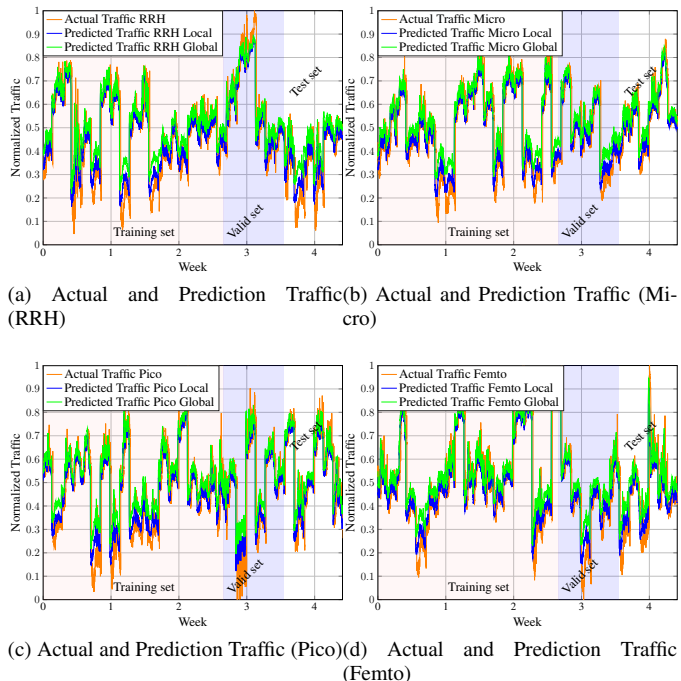


Fig. 5. Performance of the proposed federated learning based traffic prediction

TABLE IV
COMPARISON OF RMSE OF A LOCAL AND GLOBAL MODEL FOR EACH TYPE OF SBS

SBS Type	Type of Model	RMSE
RRH	Global Model	0.1221
	Local Model	0.0987
Micro	Global Model	0.1101
	Local Model	0.0902
Pico	Global Model	0.1318
	Local Model	0.1145
Femto	Global Model	0.1261
	Local Model	0.1080

would make $M_T = 144$ time slots. κ is the time conversion factor from minutes to seconds.

- **Coverage loss (C_l):** The coverage loss is a measure of the percentage difference in the total volume of traffic that is supported by the network before and after the BS switching operation is performed using the proposed and benchmark methods. The coverage loss can be expressed as:

$$C_l = \frac{\Theta^i - \Upsilon^i}{\Theta^i} \times 100\% \quad (44)$$

where Θ^i is the total traffic load of the network before BS switching and Υ^i is the total traffic of the network after BS switching operation.

D. Results and Discussions

In this section, we evaluate the performance of the proposed FAMAC framework comprising the federated learning based traffic prediction model and the modified actor-critic deep reinforcement learning based BS switching model using the performances metrics VI-C and the benchmark methods VI-B.

a) *Comparison of Traffic Prediction Techniques:* Fig 5 presents the traffic prediction performance of the local model and global federated learning model, while Table IV presents the RMSE values obtained during model training for each type of SBS in the network.

For RRHs, we can observe that the local model demonstrates better prediction accuracy than the global federated learning model, as evidenced by its lesser RMSE of 0.0987 compared to 0.1221 for the global model (Table IV). When the prediction plots in Fig. 5a are considered, the local model tracks the fluctuations in actual RRH traffic much more closely, especially in the initial training weeks. For example in week 1, the local model accurately captures a sharp rise from 0.1 to 0.8 normalized load, while the global model underestimates the surge. This is because the local model can learn unique traffic characteristics and trends specific to each RRH site. In contrast, by aggregating data across locations, the global model generalizes and misses some location-specific variations. However, as described in the paper, the global model can identify overall network-wide changes and emerging patterns in the RRH traffic (like broader increases or decreases) that local models may overlook.

For micro SBSs, again the local model attains lower prediction error (RMSE 0.0902) than the global federated model (RMSE 0.1101) as shown in Table IV. Also, from Fig. 5b, the local model consistently anticipates the ups and downs in real micro SBS traffic better across training and testing weeks. This highlights its ability to closely learn distinct micro SBS traffic behaviors that is unique to each specific location. Although less accurate locally, as explained in the paper, the global model provides advantages like privacy preservation, reduced communication overhead, adaptability to new locations, and identifying shared micro SBS traffic patterns across the network.

Regarding pico SBSs, the global and local models achieve very similar RMSE performance of 0.1318 and 0.1145 respectively, as shown in Table IV. Examining the prediction plots in Fig. 5c, both modeling approaches track the pico SBS traffic fluctuations reasonably well over the four weeks. This suggests pico SBS traffic may exhibit more homogeneous characteristics across locations. Hence for pico SBSs, the global and local models are comparable in prediction accuracy, while the global model provides benefits like privacy and reduced signaling overhead through federated learning. Finally, for femto SBSs, the global and local models again attain close RMSE values of 0.1261 and 0.1080 respectively (Table IV). As visualized in Fig. 5d, their predictions equally capture the variations in actual femto SBS traffic over the four weeks. This indicates femto SBSs experience consistent localized traffic patterns, making a specialized local model unnecessary. The global model performs on par for femto SBSs with uniform traffic, while still providing the generalization and communication efficiency benefits of federated learning.

Overall, even though the local models achieve relatively lower prediction error compared to the global model, however, the global federated learning model provides advantages like privacy, reduced signalling overhead, and adaptability, which can not be obtained when only local models are utilized.

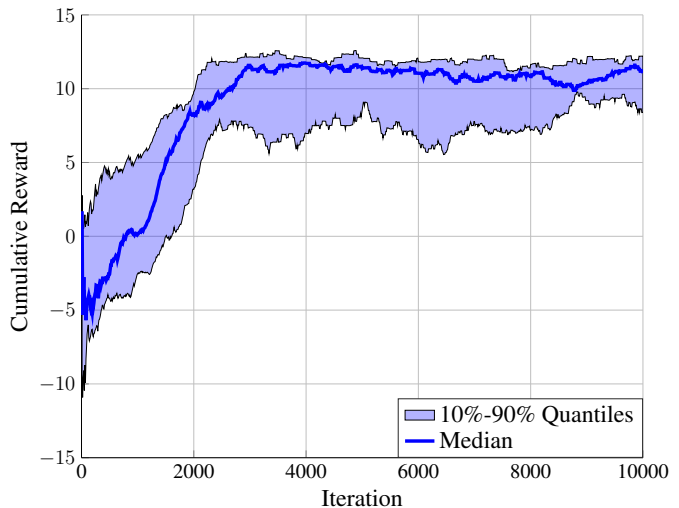


Fig. 6. Proof of Convergence curve. The darker line shows the median over seeds. We average the two extreme values to obtain the shaded area (i.e., 10% and 90% quantiles with linear interpolation).

Hence, its consideration and application in this work.

b) *Proof of Convergence:* Fig. 6 illustrates the convergence behavior of the proposed modified actor-critic deep reinforcement learning algorithm during training. The convergence curve demonstrates how the proposed modified actor-critic reinforcement learning algorithm learns an optimal BS switching policy to minimize total network power consumption using the defined reward function. The y-axis plots the reward, calculated using (40) based on current power savings and coverage constraints. A key aspect is penalizing the agent for violating the MBS traffic limit or achieving no power savings.

In the initial phase, high volatility in median reward occurs as the agent explores actions, frequently violating constraints and getting negative rewards. The wide percentile spread shows high variance across seeds as the agent struggles to find useful switch-off patterns. In the middle stage, the volatility reduces as the agent learns to satisfy constraints and achieve modest energy savings, receiving slightly positive rewards. The interquartile range narrows as performance becomes more consistent across seeds. In the final phase, the median reward increases and stabilizes close to -5 as the agent converges on optimized policies that maximize power savings without violating constraints, achieving strong positive rewards. The tight percentile spread proves the reliability of this solution across training conditions. The agent learns effective switch-off strategies tailored to traffic loads and BS types that maximize cumulative reward.

The upward trend of the median reward demonstrates the agent successfully learns to improve its policy over episodes by interacting with the environment. The feedback on power consumption and coverage loss, formalized in the reward function, enables the model to adapt its decisions to optimize the target of minimum network power. Violating constraints leads to negative rewards that teach the agent to prioritize feasibility. By repetitively testing switch-off patterns and observing results, the reinforcement learning model learns

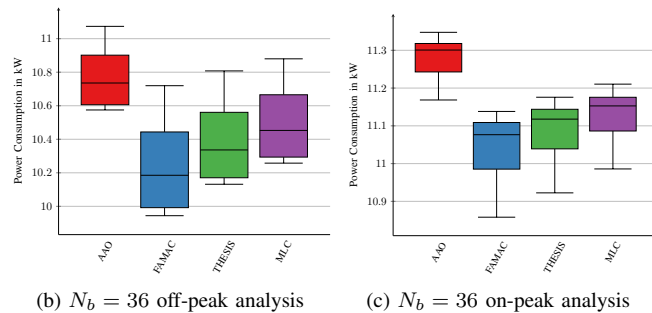
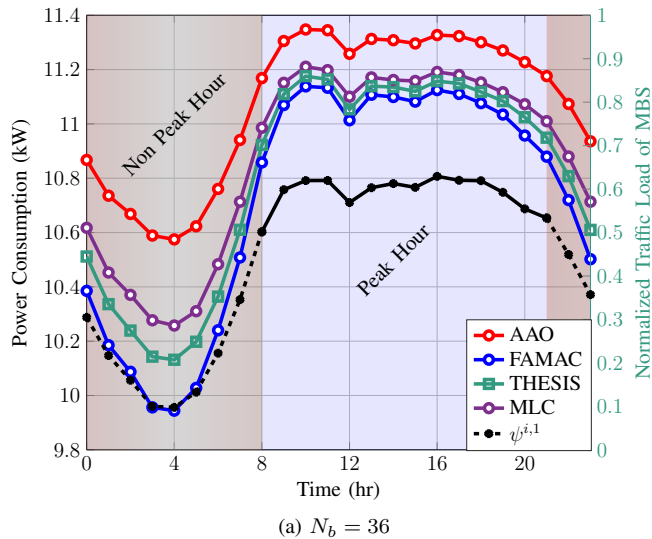


Fig. 7. Instantaneous power consumption over a 24 hrs period for 36 SBSs.

specialized intelligence to maximize power savings within operational limits. The stabilization of high median reward and narrow percentiles proves the agent has converged on an optimized solution robust to variability in training. The curve validates how the modified actor-critic approach leverages the formalized rewards to handle the immense action space and learn efficient coordinated switch-off policies that minimize energy consumption.

Ultimately, the convergence curve empirically demonstrates how the defined reward function drives learning of a reliable optimized switching policy that maximizes power reduction across the joint action space. The agent learns to satisfy QoS constraints and improve energy savings over time by interacting with the environment and receiving feedback via the designed rewards.

c) Comparison of Instantaneous power consumption:

Fig. 7a shows the instantaneous power consumption of the network over a whole day for 20 SBSs, while Fig. 7b and Fig. 7c illustrates the distribution of the instantaneous power consumption during peak and off-peak periods when the proposed and benchmark methods are implemented.

First, it can be observed from Fig. 7a that the instantaneous power consumption varies with the traffic load of the network over the 24-hour period when FAMAC and the benchmark methods are applied, that is, the power consumption is high when the traffic load is high (i.e., peak periods) and low when the traffic load is low (i.e., off-peak periods). However,

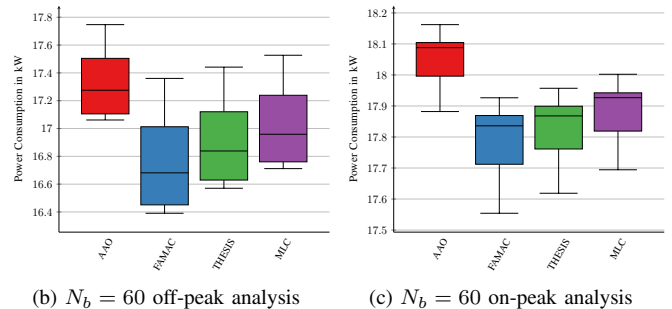
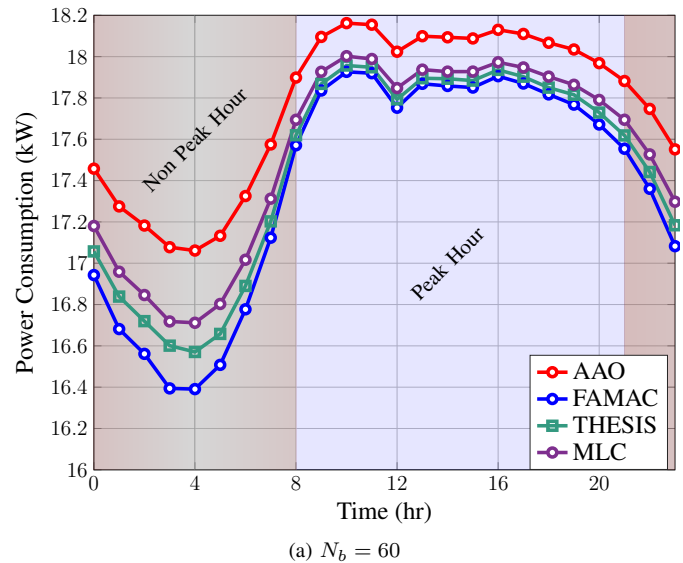


Fig. 8. Instantaneous power consumption over a 24 hrs period for 60 SBSs.

compared to the AAO where all the SBSs are on, the proposed and benchmark methods are able to reduce the power consumption of the network during both low and high traffic periods even though the magnitude of reduction in network power consumption is much higher during off-peak hours than peak hours because there are opportunities to switch off more SBSs during the former than the latter. Please note that the word offpeak and low traffic load are used interchangeably, as well as high traffic load and peak periods in this paper.

Second, a closer look at the peak and off-peak power consumption analysis as revealed by the box plots in Fig. 7b and Fig. 7c clearly reveals the superior performance of FAMAC compared to both THESIS and MLC because its median, minimum and maximum power consumption is lesser during both peak and off-peak traffic periods, even though the power consumption margin is higher at off-peak periods compared to the peak periods. The justification for the higher performance of FAMAC during offpeak compared to peak periods is that the traffic load of the network is low during offpeak periods but high during peak periods because at low traffic loads, there is more offloading capacity at the MBS and more SBSs are available to switch off, so it can carefully explore the possible combinations of SBSs to decide the option that gives the least energy consumption. However, at high traffic periods, the performance of FAMAC and the benchmark methods become similar because there is less offloading capacity in the MBS, and most SBSs are highly loaded, so the switching options

that FAMAC can select without violating the QoS constraint become very few thereby making its performance almost the same as the benchmarks at low traffic periods.

Third, from Fig. 7a, Fig. 7b and Fig. 7c, the performance of THESIS is next to that of FAMAC during both peak and offpeak periods. However, we still observe a wider margin in power consumption during low traffic periods compared to high periods. The reason for this discrepancy is that THESIS employs both clustering and exhaustive search (ES) methods which limits the amount of search spaces that the algorithm can explore to determine the optimal combination of SBSs to switch off when the traffic is low but at high traffic periods, the larger search space that FAMAC has compared to THESIS does not offer much advantage because of lack of sufficient offloading capacity at the MBS, thereby accounting for the narrow margin at high traffic load.

Fourth, it can be seen from from Fig. 7a, Fig. 7b and Fig. 7c that asides AAO, where no switching occurs, which has a lesser performance than MLC, all other methods have superior performance both during peak and off-peak periods. The rationale behind the low performance of MLC is that it does not discriminate among the different types of SBSs when deciding which SBSs to turn off and offload their traffic to the MBS. Rather, it is more concerned about switching a cluster with the highest number of SBSs whose traffic load can be accommodated by the MBS. By so doing it places more priority on the number of SBSs that can be switched off instead of the type of SBS without realizing that it is possible to consume less power when few SBSs with higher power consumption are switched off compared to when many SBSs with lesser power consumption are switched off. Hence we observe a wide margin between MLC and THESIS and a much wider margin between MLC and FAMAC during low-traffic periods. However, at high-traffic periods, the margin becomes very slim because the chances of switching off SBSs becomes very few because most of them are heavily loaded and there will also be very little offloading capacity in the MBS to accommodate their traffic load, so the uniqueness of each algorithm is barely noticed.

Fig. 8a illustrates the instantaneous power consumption of the UDHN with 60 SBSs for a 24-hour period while Fig. 8b and Fig. 8c analysis the offpeak and peak power consumption of the UDN using box plots. First, we observe a similar trend in power consumption of the network in Fig. 8a as in Fig. 7 where 36 SBSs are deployed, except that they are of power consumption values are of higher magnitude compared to that of Fig. 7. This is because more SBSs are deployed in this scenario compared to the previous scenario, thereby resulting in an increase in the overall power consumption of the network. This observation is quite intuitive because the power consumption of the network ($P_{\text{total}}(\psi_t^{i,j}, \Gamma_t^{i,j})$) is the summation of the power consumed by all the BSs that are deployed in the network as presented in (42), such that an increase in the network size would directly translate into an increase in the total power consumption of the network. The power consumption when AAO is considered is still higher than that of both the proposed and benchmark methods since no SBS is switched off, but all SBSs constantly active to cater

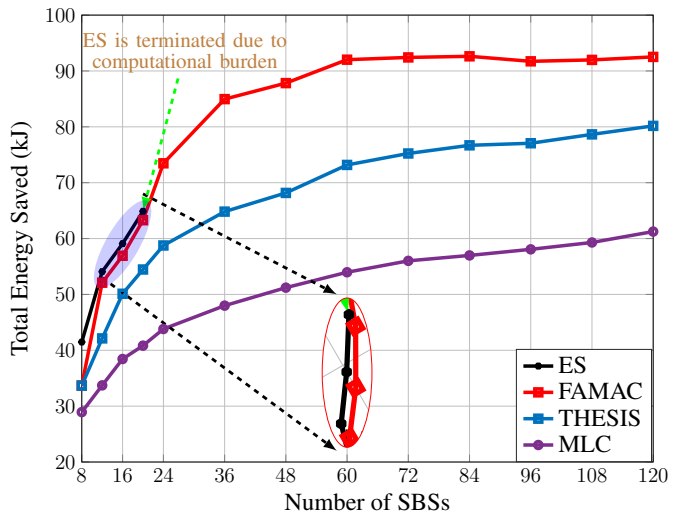


Fig. 9. Total energy saved in the UDHN for different numbers of SBSs over a 24-hour period.

to user traffic demands. As with Fig. 7, the performance of FAMAC supersedes that of THESIS and MLC much more significantly difference during periods of low traffic than high traffic because of the enhanced ability to determine the best policy in terms of the set of SBSs to select that would result in minimum energy consumption compared to THESIS and MLC. The peak and off-peak power consumption analysis with 60 SBSs as illustrated in Fig. 8b and Fig. 8c also follow a similar trend as with Fig. 7b and Fig. 7c as we also observe that FAMAC has a lesser median, minimum, and maximum power consumption values during off-peak and peak periods followed by THESIS, with MLC has the highest power consumption values which signifies it has the least performance among the BS switching algorithms.

d) Comparison of energy saving: Fig. 9 shows the variations in the amount of energy saving that can be obtained in the network when the number of SBSs increases from 8 to 120 for a 24-hour period. First, we can generally observe an increase in the amount of energy saving though with different magnitudes for all the methods between 8 and 60 SBSs, but after 60 SBS there is a decline in the magnitude of energy savings or almost steady energy savings irrespective of the increase in the number of SBSs. The rationale behind this observation is that as the number of SBSs begins to increase, there would be more opportunities to switch off more SBSs, and as a result, the energy savings begin to increase with high magnitude from 8-60 SBSs, however, from 60 SBSs upwards, the MBS seems to have become saturated such that the number of SBSs it can accommodate almost becomes constant. As such, the various switching algorithms begins to select almost the same number and type of SBSs to switch off in subsequent number of SBSs and the did in the previous number, thereby making the magnitude of energy savings with successive SBS deployment to become very small.

Second, we can observe that the ES algorithm has the best performance than FAMAC and the benchmark methods. It has a superior performance because it is able to sequentially

search through all the switching combinations to decide on the optimal number of SBSs to switch off per time, which would result in the maximum energy saving for the network. However, when the search space became very large, it becomes infeasible to sequentially search all the switching combinations to determine the optimal switching combinations because of the huge computational overhead that is involved, hence it is only feasible for small-sized networks. For this reason, we have truncated the number of SBSs for ES to 20 in this work. Third, we can see that even though the performance of FAMAC was quite lower than that of ES at 8 SBSs, from 12 to 20 SBSs, we observe an improvement in its performance with its performance being equal to that of ES at 20 SBSs. This clearly shows that FAMAC is a very close approximation of the ES and a more suitable alternative because of its scalability to the higher number of SBSs deployment with lesser computational overhead compared to ES.

Third, from Fig. 9 we can also clearly observe that FAMAC outperforms both THESIS and MLC benchmark methods in terms of energy saving. This is because it is able to take advantage of the available offloading capacity in the MBS to switch off the higher numbers and higher power-consuming type of SBSs before it saturates at about 60 SBSs. That is why we observe a much steeper increase in energy savings from 16 SBSs until about 60 SBSs where the energy savings becomes almost constant. From 60 SBSs, an increase in number of SBSs does not translate to much energy savings because the MBS is not able to accommodate more traffic from SBSs thereby making FAMAC select almost these policy from 60 SBSs onwards. The performance of THESIS is next to that of FAMAC even though its energy savings increases with a relatively lesser magnitude compared to that of FAMAC. The explanation for this happening is that THESIS is that because THESIS employs both clustering and ES approach to decide the optimal switch solutions, it is not able to consider all the SBSs in the network at once, but treats them cluster by cluster, this limits the optimality of the final switch policy that it produces. However, its performance is still better than MLC which has the worse energy saving performance because unlike MLC which tries to switch the optimal SBS cluster in the UDHN, THESIS tries to find the optimal combinations of SBSs within each cluster to switch off. By so doing, THESIS is able to select a few SBSs with higher energy consumption to switch off compared to MLC which more concerned with switching off clusters with more SBSs whose traffic load can be accommodated by the MBS. As we have elaborated in the discussions on Fig. 10, the energy savings on the network does not only depend on the number of SBSs that is turned off but also on the type of SBSs that is turned off. This means that it might be more beneficial when possible to turn off one RRH compared to 10 pico BSs because the energy saving that can be obtained from the former is much greater than the later.

Fourth, we can also infer from this figure that the deployment of more SBSs does not always translate to more SBSs being switched off because of the capacity constraints that is imposed on the network by the MBS, as it has to be able to accommodate the traffic loads of all SBSs that are to be switched off before they can be turned off. This is to

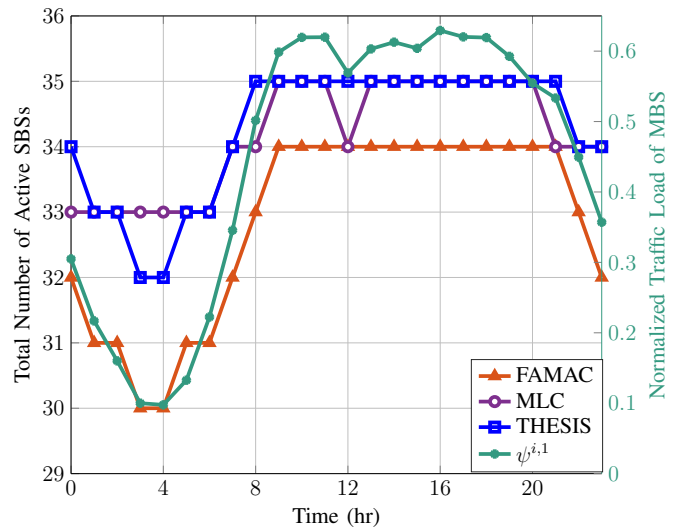


Fig. 10. A comparison of the number of active SBSs after implementing the proposed and benchmark methods.

ensure that the QoS of the network is also satisfied during BS switching. Hence, increasing the number of SBS would not always lead to an increased opportunity to switch off more SBSs which limits the amount of energy savings that can be obtained unless a provision is made to increase the offloading capacity of the MBS. Overall, it can be observed that the highest margin in energy saving between the proposed and the benchmark methods occur when 36 SBSs are deployed as the energy saving performance of FAMAC becomes 77% and 31.1% higher than THESIS and MLC, respectively.

e) Comparison of Number of active SBSs: Four major observations can be derived from Fig. 10. First, it can be clearly observed that the proposed method is specially designed to switch off more SBSs than both MLC and THESIS methods and as a result, is able to save more energy in the network compared to both benchmark methods. Second, the fact that an algorithm switches off more SBSs than another does not automatically translate to it saving more energy as can be seen when you compare Fig. 10 and Fig. 7 where even though MLC has lesser active SBSs compared to THESIS, its power consumption is still higher than that of THESIS. The reason for this is that there are four different types of SBSs deployed with varying power consumption values, so even though MLC switches off more SBS than THESIS between 3hr to 4 hr and at 12 hr, the type of SBSs being switch off is of a lesser power consumption value or a smaller SBS compared to that which THESIS switches, as such the power saving of THESIS is still superior that of THESIS. However, FAMAC has superior performance than MLC and THESIS because it is carefully designed to select not just the optimal number of SBSs but the type of SBS to switch off per time that would result in maximum energy saving in the network.

Fourth, the number of SBSs that can be turned off at any given time depends on the available capacity (number of resource blocks) at the MBS as the traffic of SBS that should be turned on must be transferred to the MBS in order to maintain the QoS. This restricts the number of SBSs that can be turned off

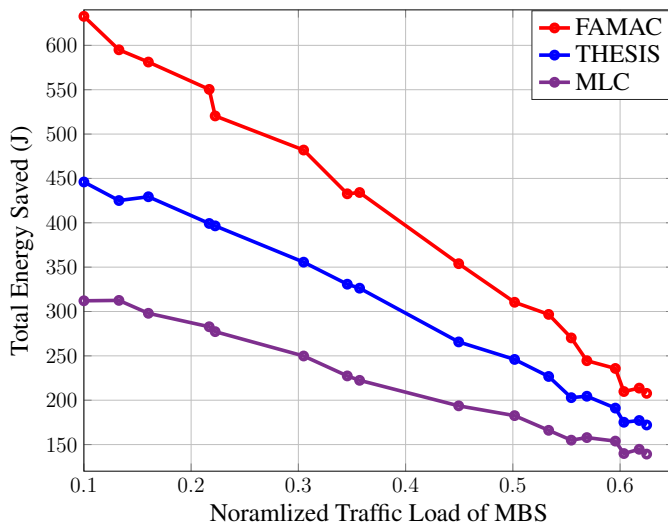


Fig. 11. The effect of the MBS traffic on the energy savings of the UDN.

and also places a limit on the amount of energy that can be saved in the network. That is why you can observe that when the traffic load of the MBS is very high from 10 hrs to 20 hrs, a maximum of two SBSs can be turned off as compared to low traffic period between 3 hr and 4hr where up to 6 SBSs can be turned off. This is because we have designed the BS switching problem in such a way that the QoS of users is given higher priority compared to the energy efficiency of the network. This is consistent with what is obtainable in practical networks as mobile network operators place more emphasis in provide quality service to their customers so as to drive up their revenue compared to turning off some SBSs to save energy. Finally, we can deduce from Fig. 10 that it is more beneficial to switch off a few SBSs with higher power consumption (e.g., RRH or micro SBSs) compared to many SBSs which have very small power consumption (e.g., femto) as the later would result in much higher energy savings compared to the later.

f) Impact of MBS traffic on energy savings: Fig. 11 illustrates the amount of energy savings that can be obtained in the network when the traffic load of the MBS varies from low to high. Here, we study the effect of the capacity constraints, that have been put in place to ensure that the QoS of the network is not violated, on the amount of energy savings that can be obtained in the network. We can clearly see that the energy saving of both the proposed and benchmark methods almost scales linearly with the amount of traffic demand on the macro-BS which means that when the MBS is lightly loaded, more energy can be saved in the network as it can accommodate more traffic load thereby allowing more SBSs to be switched off as opposed to highly loaded periods which the energy savings is very low because it can only accommodate little traffic and as such only very few SBSs can be switched off.

In addition, we can see that FAMAC outperforms both THESIS and MLC at both low and high traffic periods with energy savings of up to 99% and 42.3% greater than that of MLC and THESIS, respectively during low traffic periods. The superior performance of FAMAC is because of its ability to

select the optimal number and type of SBS(s) to switch off which will lead to maximum energy saving in the network without violating the capacity limit constraints of the MBS. Moreover, we can also see here that THESIS also performs better than MLC with an energy saving that is 40% higher than that of MLC even though MLC can switch off more SBSs than it at some time instances as observed in Fig. 10 because it has the ability to discriminate among the various types of SBSs and select the few SBS that would save a considerable amount of energy in the network. MLC has the least energy-saving performance because it is more concerned with how many SBSs can be switched off per time without considering the fact there are different types of SBS. Hence, the MLC method would be more suitable when all the SBSs in the network are of the same type.

g) Analysis of SBS power consumption: Next, we present an analysis of the instantaneous power consumption breakdown of the various types of BSs that are deployed in the network using box plot Fig. 12a to Fig. 12e for both the proposed and benchmark methods to further highlight the excellent performance of the proposed approach. The boxplot shows the median (mean), the minimum and maximum instantaneous power consumption values, and the skewness of the power consumption values which describes how the values are distributed across the mean value.

Fig. 12a depicts the distribution of the instantaneous power consumption of the RRH over a 24 hour period in the network when both the proposed and the benchmark methods are applied. We can observe that compared the case when all the RRHs are on (AAO), which is the baseline case of maximum power consumption, FAMAC has the lowest mean power consumption compared to THESIS and MLC. In addition, it has the lowest minimum power and maximum power consumption values and the power consumption values seems to be evenly distributed about the mean compared to both benchmarks THESIS and MLC where most of the power consumption values of the RRH lie above the median mark. This indicates the FAMAC seems to prioritize switching off more RRHs in the network than the other benchmarks. We can also see that THESIS has lesser mean power consumption than MLC which means it switches off more RRHs compared to MLC.

Fig. 12b presents the breakdown of the instantaneous power consumption of the micro SBSs in the network when the proposed and benchmark methods are implemented. Here, We still observe that FAMAC still has a lower mean power consumption compared to the THESIS and MLC. As for the maximum value, we see that all algorithms have almost the same maximum value while in terms of minimum value THESIS has the lowest minimum value. With respect to data skewness, the power consumption values of FAMAC are evenly distributed around the mean while most of the power consumption value of THESIS and MLC lie above the median value. From these observations, we still see that the performance of FAMAC is still slightly FAMAC better in terms of prioritizing the switching off of more micro SBSs compared to THESIS and MLC while the performance of THESIS and MLC is almost the same even though the

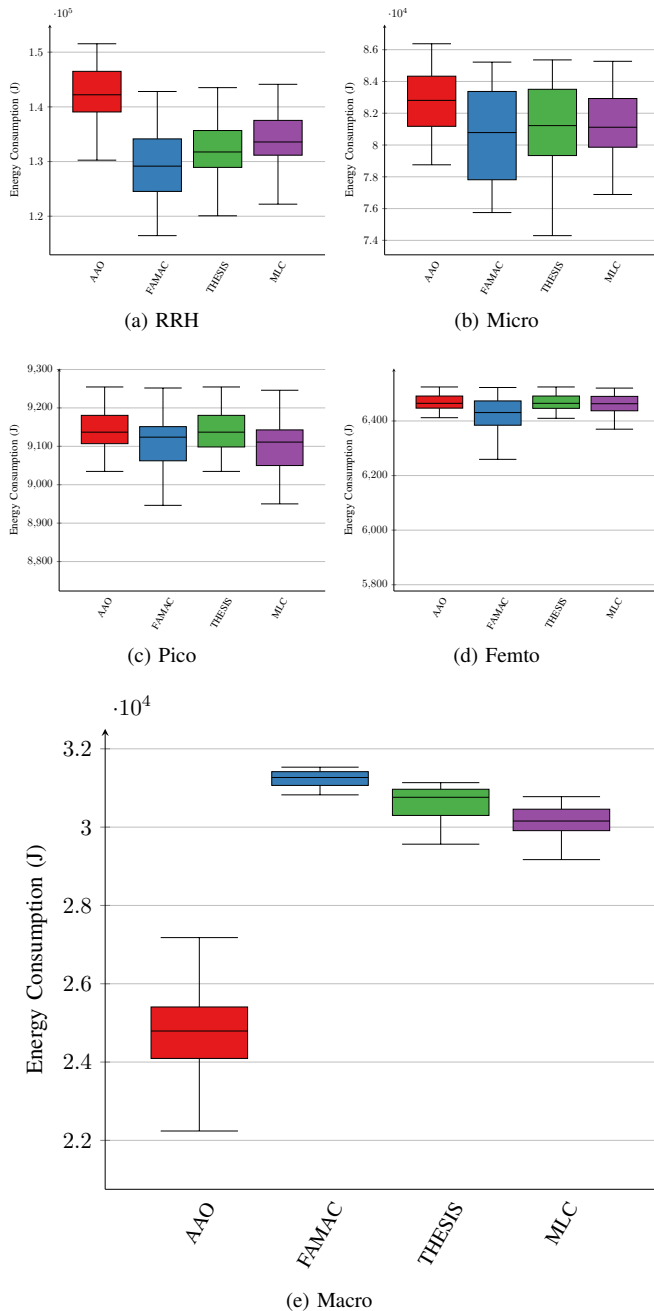


Fig. 12. Comparison of the energy consumption breakdown of the different types of BSs in the network for 36 SBSs when the proposed and benchmark methods are applied.

minimum power consumption value of THESIS is less than that of MLC.

Fig. 12c shows the median, minimum, maximum and skewness of the instantaneous power consumption values of the pico SBSs in the network when the proposed and benchmark methods are applied. It can be observed that the MLC has a slightly lower median power consumption compared to FAMAC, while THESIS has higher median power consumption than both FAMAC and MLC. In terms of minimum and maximum power consumption, both MLC and FAMAC have the same minimum power consumption, with the maximum

value of MLC slightly less than that of THESIS. THESIS has the same maximum value as FAMAC, but its minimum value is much higher than MLC and THESIS. For power consumption skewness, most of the power consumption values of THESIS and MLC are lower than the median market, while that of THESIS is evenly distributed around the median. These observations suggest that MLC gives more priority to switching off pico SBSs, followed by FAMAC, while THESIS seems not to switch off any pico SBS as its median, maximum, and minimum power consumption values are almost the same as that of AAO, which is the case where all pico SBSs are kept on. Fig. 12d presents the power consumption break for Femto SBSs. Here we can see that FAMAC has a lower median and minimum power consumption compared to THESIS and MLC, even though both the proposed and benchmark methods have the same maximum value. The performance of MLC is almost the same as that of THESIS, but it has a slightly lesser median, minimum power consumption value compared to THESIS. Here again, we see that THESIS has the same performance as AAO which indicates that no femto SBS was turned off when THESIS was applied to the network with 36 SBSs.

Fig. 12e shows the median, minimum and maximum power consumption values of the macro BS when FAMAC, THESIS, MLC, and AAO are applied. It can be seen that all the power consumption values of the macro BS with AAO, when all the BSs are on, are the least and FAMAC has the highest power consumption. The rationale behind this is that, with FAMAC, more SBSs can be turned off (as we see in Fig 10), which means that more traffic is offloaded from the SBSs to the macro, and this translates to higher energy consumption in the network. The power consumption of THESIS follows that of FAMAC because, as we can see from Fig. 12a to Fig. 12d, THESIS switches off more RRH and micro SBSs which have more capacity (resource blocks) and power consumption compared to MLC and as result is able to offload more traffic to the MBS which results in higher energy consumption compared to that of the MLC, even though from Fig 10, it turns off a lesser number of SBSs compared to MLC. MLC has the lowest power consumption in the MBS because it prioritizes switching off more pico and femto SBS, which are off lesser capacity and power consumption than micro and RRH, as a result, the amount of offloaded traffic is lesser than that of THESIS and FAMAC which also leads to lesser energy consumption in the network.

Overall, when we analyse the performance of the proposed and benchmark algorithms with respect to the type of SBSs they prefer to switch off as well as their corresponding power consumption statistics from Fig. 12a to Fig. 12e, we can clearly observe that FAMAC outperforms the benchmark methods. This is because it gives priority to SBSs with higher power consumption values (RRH and micro SBSs) during BS switching, without neglecting to switch off smaller power consumption (pico and femto SBSs). This also accounts for why it mostly has the lowest median, maximum and minimum power consumption values among the four types of SBSs considered. In addition, We see that THESIS only switches off RRHs and Micro SBSs while leaving pico and femto

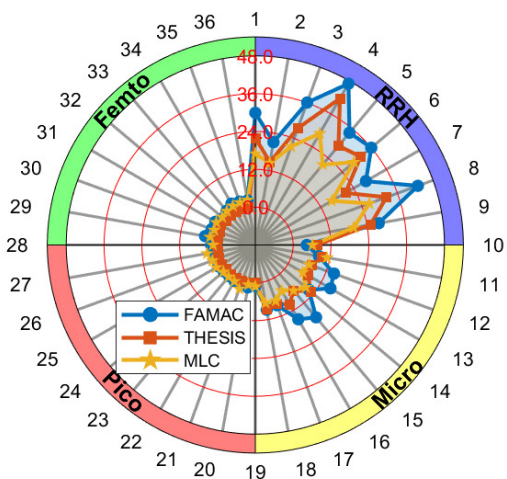


Fig. 13. Polar plot illustrating the average daily switch-off occurrences for each base station type using proposed and benchmark methods. The plot encompasses 36 small cells, with nine instances of the following base station types: RRH, Micro, Pico, and Femto.

SBS mostly on, which makes its performance next to that of FAMAC. MLC has the least performance because, even though it tries to turn off each type of SBS at each switching instance, it tends to turn off more SBSs with smaller power consumption (pico and femto SBSs) compared to those with larger power consumption (RRHs and micro SBSs). However, when it comes to the MBS, the reverse is the case as MLC has the lower power consumption among the benchmark methods followed by THESIS, and FAMAC has the highest power consumption because the more SBSs you turn off, the more traffic you offload to the MBS, and the higher the power consumption of the MBS. FAMAC has higher power consumption in the macro because it turns off more SBSs and prioritizes the turning off of SBSs with higher capacity and power consumption profile compared to MLC and THESIS.

h) Analysis of switch-off occurrence among SBSs: We further demonstrate the superior performance of the proposed framework using a polar plot as illustrated in Fig. 13, which compares the average daily switch-off occurrences for the different SBS types. The plot shows results for a network with 36 SBSs, with 9 SBSs of each type. The polar plot has four quarters, each representing a SBS type (i.e., 1-9 RRHs, 10-18 micro SBSs, 19-27 pico SBSs, and 28-36 femto SBSs). Within each quarter, there are radii, each 10 degrees apart, which denote the number of each type of SBS, and concentric circles, which indicate the average frequency of switch off of each SBS type when FAMAC, THESIS and MLC are implemented.

We can see FAMAC switches off around 7 out of 9 RRH, 5 out of 9 micro SBSs, and for Pico and Femto SBSs, only 2-3 out of 9 are switched off on average. So FAMAC preferentially switches off more RRH and Micro SBSs compared to Pico and Femto SBSs. By targeting high power consumption SBSs, FAMAC is able to maximize energy savings since RRH and Micro SBSs have higher power consumption compared to Pico and Femto. This is because switching off 1 RRH saves more energy than switching off several Pico/Femto SBSs. The polar plot also indicates that THESIS is able to switch off a moderate

number of RRH and Micro SBSs. However, it rarely switches off Pico and Femto SBSs. This is consistent with the analysis in the paper that THESIS focuses on selective switch-off of high-power SBSs because its hybrid approach prevents it from exploring the full search space, thereby limiting its overall energy savings. The plot shows that MLC has a more balanced switching across RRH, Micro, Pico, and Femto SBSs, but the number of SBSs switched off is lower overall compared to FAMAC. However, because it does not target the switching off of more SBSs with high power consumption than THESIS or FAMAC, it is not able to maximize power reduction, thereby resulting in its lowest performance.

i) Coverage loss analysis: It should be noted that the due to the way the BS switching problem was formulated in this work, both the proposed and benchmark methods have been designed and implemented in such a way that we paid more stringent attention to the QoS constraint (12) during simulations by ensuring that the traffic of users associated with SBSs that are to be turned off are always re-associated with the MBS before turning them off. As a result, the coverage loss of FAMAC, THESIS, and MLC are the same (i.e., the coverage loss obtained from all methods is zero, which is the case where the traffic demand before and after BS switching was implemented is the same). We adopted this approach when designing and implementing the proposed and benchmark methods because we understand that in practical networks, MNOs emphasise satisfying user service demands rather than sacrificing user QoS to save energy in the network. This is because the more users are satisfied with their service, the more they would patronize that service, which would lead to revenue growth. Hence, even though the energy-saving technique we proposed in this paper would reduce operating expenses, the MNOs would be more open to embracing a BS-switching approach that would save energy and cost while not degrading the QoS provided to the network users.

In summary, extensive evaluations based on real-world traffic data showed that FAMAC could adaptively determine highly optimized BS switch-off patterns across time by exploiting the capabilities of federated learning for distributed privacy-preserving traffic prediction and a tailored actor-critic deep RL algorithm to handle constraints and large discrete action spaces inherent in ultra-dense 5G networks. The proposed innovations enabled learning coordinated, intelligent switching policies to minimize network energy consumption across both peak and off-peak periods while always satisfying quality of service guarantees by serving all user traffic. Our results proved FAMAC's ability to outperform existing approaches.

VII. CONCLUSION

In this work, we considered the energy optimisation problem in 5G and beyond cellular networks comprising ultra-dense heterogeneous BS deployment to obtain a sustainable and cost-efficient network. To achieve this, we proposed a proactive and intelligent energy-saving framework where the future traffic of the BSs is determined beforehand in a secure manner using federated learning followed by the application of a modified version of the actor-critic DRL algorithm to determine the best

switching policy that would lead to maximum energy saving in the network. The performance evaluations revealed that the proposed framework could save significant energy compared to state-of-the-art solutions while respecting the quality of service constraints. In addition, it is also scalable, which means that it can be applied to 5G and beyond networks even when their dimension becomes very large. In the future, we would consider various techniques for enhancing the offloading capacity of the macro BS in order to give room for more small BSs to be turned off, thereby improving the amount of energy savings that can be obtained in the network.

REFERENCES

- [1] M. A. Adedoyin and O. E. Falowo, "Combination of ultra-dense networks and other 5G enabling technologies: A survey," *IEEE Access*, vol. 8, pp. 22 893–22 932, jan 2020.
- [2] O. Alamu, A. Gbenga-Ilori, M. Adelabu, A. Imoize, and O. Ladipo, "Energy efficiency techniques in ultra-dense wireless heterogeneous networks: An overview and outlook," *Engineering Science and Technology, an International Journal*, vol. 23, no. 6, pp. 1308 – 1326, dec 2020. [Online]. Available: <http://www.sciencedirect.com/science/article/pii/S2215098619328745>
- [3] Y. Xu, G. Gui, H. Gacanin, and F. Adachi, "A survey on resource allocation for 5G heterogeneous networks: Current research, future trends, and challenges," *IEEE Communications Surveys Tutorials*, vol. 23, no. 2, pp. 668–695, feb 2021.
- [4] Nidhi and A. Mihovska, "Small cell deployment challenges in ultradense networks: Architecture and resource management," in *2020 12th International Symposium on Communication Systems, Networks and Digital Signal Processing (CSNDSP)*, jul 2020, pp. 1–6.
- [5] M. Usama and M. Erol-Kantarci, "A survey on recent trends and open issues in energy efficiency of 5G," *Sensors*, vol. 19, no. 14, p. 3126, jul 2019.
- [6] S. Buzzi, C.-L. I, T. E. Klein, H. V. Poor, C. Yang, and A. Zappone, "A survey of energy-efficient techniques for 5G networks and challenges ahead," *IEEE Journal on Selected Areas in Communications*, vol. 34, no. 4, pp. 697–709, apr 2016.
- [7] J. Wu, Y. Zhang, M. Zukerman, and E. K.-N. Yung, "Energy-efficient base-stations sleep-mode techniques in green cellular networks: A survey," *IEEE Communications Surveys and Tutorials*, vol. 17, no. 2, pp. 803–826, 2015.
- [8] R. Aslani and M. Rasti, "A distributed power control algorithm for energy efficiency maximization in wireless cellular networks," *IEEE Wireless Communications Letters*, vol. 9, no. 11, pp. 1975–1979, jul 2020.
- [9] S. Morosi, E. Del Re, and P. Piunti, "Traffic based energy saving strategies for green cellular networks," in *European Wireless 2012; 18th European Wireless Conference 2012*, 2012, pp. 1–6.
- [10] L. A. Ferhi, K. Sethom, and F. Choubani, "Toward dynamic 3D sectorization using real traffic profile for green 5G cellular networks," in *2018 International Conference on Advanced Systems and Electric Technologies (IC_ASET)*, mar 2018, pp. 227–232.
- [11] A. I. Abubakar, M. Ozturk, S. Hussain, and M. A. Imran, "Q-learning assisted energy-aware traffic offloading and cell switching in heterogeneous networks," in *2019 IEEE 24th International Workshop on Computer Aided Modeling and Design of Communication Links and Networks (CAMAD)*, sep 2019, pp. 1–6.
- [12] A. E. Amine, P. Dini, and L. Nuaymi, "Reinforcement learning for delay-constrained energy-aware small cells with multi-sleeping control," in *2020 IEEE International Conference on Communications Workshops (ICC Workshops)*, jul 2020, pp. 1–6.
- [13] J. O. Ogbobor, A. L. Imoize, and A. A.-A. Atayero, "Energy efficient design techniques in next-generation wireless communication networks: Emerging trends and future directions," *Wireless Communications and Mobile Computing*, vol. 2020, mar 2020.
- [14] F. Han, S. Zhao, L. Zhang, and J. Wu, "Survey of strategies for switching off base stations in heterogeneous networks for greener 5G systems," *IEEE Access*, vol. 4, pp. 4959–4973, aug 2016.
- [15] M. Feng, S. Mao, and T. Jiang, "Base station ON-OFF switching in 5G wireless networks: Approaches and challenges," *IEEE Wireless Communications*, vol. 24, no. 4, pp. 46–54, aug 2017.
- [16] M. Ozturk, A. I. Abubakar, J. P. B. Nadas, R. N. B. Rais, S. Hussain, and M. A. Imran, "Energy optimization in ultra-dense radio access networks via traffic-aware cell switching," *IEEE Transactions on Green Communications and Networking*, pp. 1–1, feb 2021.
- [17] A. I. Abubakar, M. S. Mollel, M. Ozturk, S. Hussain, and M. A. Imran, "A lightweight cell switching and traffic offloading scheme for energy optimization in ultra-dense heterogeneous networks," *Physical Communication*, vol. 52, p. 101643, 2022.
- [18] N. Bui, M. Cesana, S. A. Hosseini, Q. Liao, I. Malanchini, and J. Widmer, "A Survey of Anticipatory Mobile Networking: Context-Based Classification, Prediction Methodologies, and Optimization Techniques," *IEEE Communications Surveys Tutorials*, vol. 19, no. 3, pp. 1790–1821, thirdquarter 2017.
- [19] Y. Yuan, L. Lei, T. X. Vu, S. Chatzinotas, S. Sun, and B. Ottersten, "Energy minimization in uav-aided networks: Actor-critic learning for constrained scheduling optimization," *IEEE Transactions on Vehicular Technology*, vol. 70, no. 5, pp. 5028–5042, 2021.
- [20] K. Lin and J. Zhang, "Energy efficiency enhancement via power modification with simulated annealing cell selection," in *2018 IEEE 8th Annual Computing and Communication Workshop and Conference (CCWC)*, 2018, pp. 526–531.
- [21] L. Mortazavi, M. Alishahi, A. R. Darbandiolya, and A. M. Nazemi, "Turn off/on base stations with cso approach using simulated annealing algorithm in 5g networks," in *2020 10th International Conference on Computer and Knowledge Engineering (ICCKE)*, 2020, pp. 660–664.
- [22] H. Fourati, R. Maaloul, L. Fourati, and M. Jmaiel, "An efficient energy-saving scheme using genetic algorithm for 5g heterogeneous networks," *IEEE Systems Journal*, vol. 17, no. 1, pp. 589–600, 2023.
- [23] J. J. Espinosa-Martínez, J. Galeano-Brajones, J. Carmona-Murillo, and F. Luna, "Binary particle swarm optimization for selective cell switch-off in ultra-dense 5g networks," in *Swarm Intelligence: 13th International Conference, ANTS 2022, Málaga, Spain, November 2–4, 2022, Proceedings*. Springer, 2022, pp. 275–283.
- [24] M. Osama, S. El Ramly, and B. Abdelhamid, "Binary pso with classification trees algorithm for enhancing power efficiency in 5g networks," *Sensors*, vol. 22, no. 21, p. 8570, 2022.
- [25] M. H. Alsharif, A. H. Kelechi, J. Kim, and J. H. Kim, "Energy efficiency and coverage trade-off in 5g for eco-friendly and sustainable cellular networks," *Symmetry*, vol. 11, no. 3, p. 408, 2019.
- [26] N. Saxena, A. Roy, and H. Kim, "Traffic-aware cloud ran: A key for green 5g networks," *IEEE Journal on Selected Areas in Communications*, vol. 34, no. 4, pp. 1010–1021, 2016.
- [27] L. Li, N. Deng, and W. Zhou, "Environment-aware dynamic management for energy saving in mimo-based c-ran," *IEEE Access*, vol. 7, pp. 77 514–77 523, 2019.
- [28] F. Luna, P. H. Zapata-Cano, J. C. Gonzalez-Macias, and J. F. Valenzuela-Valdés, "Approaching the cell switch-off problem in 5g ultra-dense networks with dynamic multi-objective optimization," *Future Generation Computer Systems*, vol. 110, pp. 876–891, 2020.
- [29] J. Galeano-Brajones, F. Luna-Valero, J. Carmona-Murillo, P. H. Z. Cano, and J. F. Valenzuela-Valdés, "Designing problem-specific operators for solving the cell switch-off problem in ultra-dense 5g networks with hybrid moeas," *Swarm and Evolutionary Computation*, p. 101290, 2023.
- [30] N. Bui, M. Cesana, S. A. Hosseini, Q. Liao, I. Malanchini, and J. Widmer, "A survey of anticipatory mobile networking: Context-based classification, prediction methodologies, and optimization techniques," *IEEE Communications Surveys Tutorials*, vol. 19, no. 3, pp. 1790–1821, apr 2017.
- [31] F. Hussain, S. A. Hassan, R. Hussain, and E. Hossain, "Machine learning for resource management in cellular and IoT networks: Potentials, current solutions, and open challenges," *IEEE Communications Surveys Tutorials*, vol. 22, no. 2, pp. 1251–1275, jan 2020.
- [32] A. I. Abubakar, M. Ozturk, R. N. B. Rais, S. Hussain, and M. A. Imran, "Load-aware cell switching in ultra-dense networks: An artificial neural network approach," in *2020 International Conference on UK-China Emerging Technologies (UCET)*, aug 2020, pp. 1–4.
- [33] L. Wang, S. Chen, and M. Pedram, "Context-driven power management in cache-enabled base stations using a bayesian neural network," in *2017 Eighth International Green and Sustainable Computing Conference (IGSC)*, oct 2017, pp. 1–8.
- [34] I. Donevski, G. Vallero, and M. A. Marsan, "Neural networks for cellular base station switching," in *IEEE INFOCOM 2019 - IEEE Conference on Computer Communications Workshops (INFOCOM WKSHPS)*, 2019, pp. 738–743.
- [35] K. Tan, D. Bremner, J. Le Kernec, Y. Sambo, L. Zhang, and M. A. Imran, "Graph neural network-based cell switching for energy optimization in

- ultra-dense heterogeneous networks,” *Scientific Reports*, vol. 12, no. 1, p. 21581, 2022.
- [36] J. Li, H. Wang, X. Wang, and Z. Li, “Optimized sleep strategy based on clustering in dense heterogeneous networks,” *EURASIP Journal on Wireless Communications and Networking*, vol. 2018, no. 1, pp. 1–10, dec 2018.
- [37] S. M. Asad, S. Ansari, M. Ozturk, R. N. B. Rais, K. Dashtipour, S. Hussain, Q. H. Abbasi, and M. A. Imran, “Mobility management-based autonomous energy-aware framework using machine learning approach in dense mobile networks,” *Signals*, vol. 1, no. 2, pp. 170–187, nov 2020. [Online]. Available: <https://www.mdpi.com/2624-6120/1/2/10>
- [38] A. I. Abubakar, M. Ozturk, S. Hussain, and M. A. Imran, “Q-Learning Assisted Energy-Aware Traffic Offloading and Cell Switching in Heterogeneous Networks,” in *2019 IEEE 24th International Workshop on Computer Aided Modeling and Design of Communication Links and Networks (CAMAD)*, Sep. 2019, pp. 1–6.
- [39] Q. Zhang, X. Xu, J. Zhang, X. Tao, and C. Liu, “Dynamic load adjustments for small cells in heterogeneous ultra-dense networks,” in *2020 IEEE Wireless Communications and Networking Conference (WCNC)*, may 2020, pp. 1–6.
- [40] A. E. Amine, J.-P. Chaiban, H. A. H. Hassan, P. Dini, L. Nuaymi, and R. Achkar, “Energy optimization with multi-sleeping control in 5g heterogeneous networks using reinforcement learning,” *IEEE Transactions on Network and Service Management*, vol. 19, no. 4, pp. 4310–4322, 2022.
- [41] A. El-Amine, H. A. Haj Hassan, M. Iturralde, and L. Nuaymi, “Location-aware sleep strategy for energy-delay tradeoffs in 5g with reinforcement learning,” in *2019 IEEE 30th Annual International Symposium on Personal, Indoor and Mobile Radio Communications (PIMRC)*, 2019, pp. 1–6.
- [42] X. Huang, S. Tang, D. Zhang, and Q. Chen, “Cluster-based dynamic FBSs on/off scheme in heterogeneous cellular networks,” in *International Conference on Communications and Networking in China*. Springer, jan 2018, pp. 325–335.
- [43] C.-Q. Dai, B. Fu, and Q. Chen, “A cluster-based small cell on/off scheme for energy efficiency optimization in ultra-dense networks,” in *International Conference on Communications and Networking in China*. Springer, feb 2019, pp. 385–401.
- [44] R. S. Sutton and A. G. Barto, *Reinforcement learning: An introduction*. MIT press, 2018.
- [45] J. Liu, B. Krishnamachari, S. Zhou, and Z. Niu, “DeepNap: Data-driven base station sleeping operations through deep reinforcement learning,” *IEEE Internet of Things Journal*, vol. 5, no. 6, pp. 4273–4282, dec 2018.
- [46] K. Zhang, X. Wen, Y. Chen, and Z. Lu, “Deep reinforcement learning for energy saving in radio access network,” in *2020 IEEE/CIC International Conference on Communications in China (ICCC Workshops)*, aug 2020, pp. 35–40.
- [47] C. Huang and P. Chen, “Joint demand forecasting and DQN-based control for energy-aware mobile traffic offloading,” *IEEE Access*, vol. 8, pp. 66 588–66 597, apr 2020.
- [48] R. Li, Z. Zhao, X. Chen, J. Palicot, and H. Zhang, “TACT: A transfer actor-critic learning framework for energy saving in cellular radio access networks,” *IEEE Transactions on Wireless Communications*, vol. 13, no. 4, pp. 2000–2011, apr 2014.
- [49] S. Sharma, S. J. Darak, and A. Srivastava, “Energy saving in heterogeneous cellular network via transfer reinforcement learning based policy,” in *2017 9th International Conference on Communication Systems and Networks (COMSNETS)*, 2017, pp. 397–398.
- [50] Q. Wu, X. Chen, Z. Zhou, L. Chen, and J. Zhang, “Deep reinforcement learning with spatio-temporal traffic forecasting for data-driven base station sleep control,” *IEEE/ACM Transactions on Networking*, vol. 29, no. 2, pp. 935–948, jan 2021.
- [51] J. Ye and Y.-J. A. Zhang, “Drag: Deep reinforcement learning based base station activation in heterogeneous networks,” *IEEE Transactions on Mobile Computing*, vol. 19, no. 9, pp. 2076–2087, 2020.
- [52] V. Mnih, K. Kavukcuoglu, D. Silver, A. A. Rusu, J. Veness, M. G. Bellemare, A. Graves, M. Riedmiller, A. K. Fidjeland, G. Ostrovski *et al.*, “Human-level control through deep reinforcement learning,” *nature*, vol. 518, no. 7540, pp. 529–533, 2015.
- [53] M. S. Mollé, S. Kaijage, M. Kisangiri, M. A. Imran, and Q. H. Abbasi, “Multi-user position based on trajectories-aware handover strategy for base station selection with multi-agent learning,” in *2020 IEEE International Conference on Communications Workshops (ICC Workshops)*, June 2020, pp. 1–6.
- [54] I. Donevski, G. Vallero, and M. A. Marsan, “Neural networks for cellular base station switching,” in *IEEE INFOCOM 2019 - IEEE Conference on Computer Communications Workshops (INFOCOM WKSHPS)*, 2019, pp. 738–743.
- [55] G. Auer, V. Giannini, C. Desset, I. Godor, P. Skillermark, M. Olsson, M. Imran, D. Sabella, M. Gonzalez, O. Blume, and A. Fehske, “How much energy is needed to run a wireless network?” *IEEE Wireless Communications*, vol. 18, no. 5, pp. 40–49, oct 2011.
- [56] B. Debaillie, C. Desset, and F. Louagie, “A flexible and future-proof power model for cellular base stations,” in *2015 IEEE 81st Vehicular Technology Conference (VTC Spring)*. IEEE, may 2015.
- [57] A. R. Khan, I. Ahmed, L. Mohjazi, S. Hussain, R. N. B. Rais, M. A. Imran, and A. Zoha, “Latency-aware blockage prediction in federated vision-aided wireless communication,” *Frontiers in Communications and Networks*, 2023.
- [58] M. H. Mahmoud, A. Albaseer, M. Abdallah, and N. Al-Dhahir, “Federated learning resource optimization and client selection for total energy minimization under outage, latency, and bandwidth constraints with partial or no csi,” *IEEE Open Journal of the Communications Society*, vol. 4, pp. 936–953, 2023.
- [59] J. Konečný, B. McMahan, and D. Ramage, “Federated Optimization: Distributed Optimization Beyond the Datacenter,” *arXiv e-prints*, p. arXiv:1511.03575, Nov. 2015.
- [60] C. Zhang, S. Dang, B. Shihada, and M.-S. Alouini, “Dual attention-based federated learning for wireless traffic prediction,” in *IEEE INFOCOM 2021 - IEEE Conference on Computer Communications*, 2021, pp. 1–10.
- [61] H. B. McMahan, E. Moore, D. Ramage, S. Hampson, and B. Agüera y Arcas, “Communication-Efficient Learning of Deep Networks from Decentralized Data,” *arXiv e-prints*, p. arXiv:1602.05629, Feb. 2016.
- [62] F. A. Gers, J. Schmidhuber, and F. Cummins, “Learning to forget: Continual prediction with lstm,” *Neural Computation*, vol. 12, no. 10, pp. 2451–2471, 2000.
- [63] A. Graves, A.-r. Mohamed, and G. Hinton, “Speech Recognition with Deep Recurrent Neural Networks,” *arXiv e-prints*, p. arXiv:1303.5778, Mar. 2013.
- [64] J. Schulman, P. Moritz, S. Levine, M. Jordan, and P. Abbeel, “High-Dimensional Continuous Control Using Generalized Advantage Estimation,” *arXiv e-prints*, p. arXiv:1506.02438, Jun. 2015.
- [65] G. Barlacchi, M. De Nadai, R. Larcher, A. Casella, C. Chitic, G. Torrissi, F. Antonelli, A. Vespignani, A. Pentland, and B. Lepri, “A multi-source dataset of urban life in the city of milan and the province of trentino,” *Scientific data*, vol. 2, p. 150055, oct 2015.